İsmail Emre YAĞMUR
M.Sc. Thesis
AGU 2024

INVESTIGATING THE ORIGIN OF THE WEEKLY CYCLE DURING THE COVID-19 VIRUS PANDEMIC AND ITS RELATION TO SOCIO-ECONOMIC FACTORS

M.Sc. THESIS
SUBMITTED TO THE DEPARTMENT OF BIOENGINEERING AND THE GRADUATE SCHOOL OF ENGINEERING AND SCIENCE OF ABDULLAH GUL UNIVERSITY IN PARTIAL FULFILLMENT OF THE REQUIREMENTS FOR THE DEGREE OF MASTER OF SCIENCE

By
İsmail Emre YAĞMUR
January 2024

INVESTIGATING THE ORIGIN OF THE WEEKLY CYCLE DURING THE COVID-19 VIRUS PANDEMIC AND ITS RELATION TO SOCIO-ECONOMIC FACTORS

M.Sc. THESIS

SUBMITTED TO THE DEPARTMENT OF BIOENGINEERING AND THE GRADUATE SCHOOL OF ENGINEERING AND SCIENCE OF ABDULLAH GUL UNIVERSITY IN PARTIAL FULFILLMENT OF THE REQUIREMENTS FOR

THE DEGREE OF MASTER OF SCIENCE

By

İsmail Emre YAĞMUR

January 2024

SCIENTIFIC ETHICS COMPLIANCE

I hereby declare that all information in this document has been obtained in accordance with academic rules and ethical conduct. I also declare that, as required by these rules and conduct, I have fully cited and referenced all materials and results that are not original to this work.

Name-Surname: İsmail Emre YAĞMUR

Signature:

REGULATORY COMPLIANCE

M.Sc. thesis titled “Investigating The Origin of The Weekly Cycle During The COVID-19 Virus Pandemic and Its Relation to Socio-economic Factors” has been prepared in accordance with the Thesis Writing Guidelines of the Abdullah Gül University, Graduate School of Engineering & Science.

Prepared By	Advisor
İsmail. Emre YAĞMUR	Asst. Prof. Altan ERCAN

Head of the Bioengineering Program
Asst. Prof. Altan ERCAN

ACCEPTANCE AND APPROVAL

M.Sc. thesis titled “Investigating The Origin of The Weekly Cycle During The COVID-19 Virus Pandemic and Its Relation to Socio-economic Factors” and prepared by İsmail Emre YAĞMUR has been accepted by the jury in the Bioengineering Graduate Program at Abdullah Gül University, Graduate School of Engineering & Science.

26 /01/ 2024

(Thesis Defense Exam Date)

JURY:

Advisor: (Assist. Prof. Altan ERCAN) …….....

Member: (Doç. Dr. Aysun ADAN) …….....

Member: (Prof. Dr. Ahmet ÖZTÜRK) …….....

APPROVAL:

The acceptance of this M.Sc. thesis has been approved by the decision of the Abdullah Gül University, Graduate School of Engineering & Science, Executive Board dated ….. /….. / …….. and numbered ……..…… .

…….. /…….. / ……..

(Date)

Graduate School Dean

Prof. İrfan ALAN

ABSTRACT

Investigating The Origin of The Weekly Cycle During The COVID-19 Virus Pandemic and Its Relation to Socio-economic Factors

İsmail Emre YAĞMUR

MSc. In Bioengineering

Advisor: Asst. Prof. ALTAN ERCAN

January 2024

The Covid-19 virus, which started in China in 2019 and affected the whole world, has caused a global pandemic. Looking at the worldwide data of this pandemic, the number of daily cases appears to have a weekly cycle that is underestimated as an artifact of the number of daily tests administered. In this thesis study, a new model is developed to calculate the daily infection numbers from daily case numbers by using the Weibull distribution and the natural characteristics of the COVID-19 virus. According to the results obtained, it is found that the number of daily cases has a real weekly cycle. It has been determined that the daily infection numbers calculated in this weekly cycle are minimum on weekdays. According to the analysis by the new methos, these weekly minimums are controlled by socio-economic factors such as human development index and annual national income per capita. During the ascending and descending phases of the pandemic, the weekly minimum shifts from Monday to Friday, exposing the presence of two separate environments for the transmission of the virus among people: working and social. Moreover, the data reveal a variable rather than a fixed reproduction number. As a result, the model we developed in this study successfully identifies the socio-economic factors as the effectors of the progression of the pandemic by taking into account the time of infection for the first time in the literature and is expected to guide the future pandemic studies and pandemic, itself.

Keywords: SARS-CoV-2, COVID-19, Infection Time and Number, Weekly Cycle.

ÖZET

COVID-19 Virüs Pandemisinde Haftalık Döngünün Kökeni ve Sosyo-Ekonomik Faktörlerle İlişkisinin Araştırılması

İsmail Emre YAĞMUR
Biyomühendislik Anabilim Dalı Yüksek Lisans
Danışman: Dr. Öğr. Üyesi ALTAN ERCAN
Ocak 2024

2019 yılında Çin'de başlayıp tüm dünyayı etkisi altına alan Kovid-19 virüsü, küresel bir salgına neden oldu. Bu salgının dünya çapındaki verilerine bakıldığında, günlük vaka sayısının, uygulanan günlük test sayısının bir eseri olarak hafife alınan haftalık bir döngüye sahip olduğu görülmektedir. Bu araştırmada, Weibull dağılımı ve COVID-19 virüsünün özellikleri kullanılarak günlük vaka sayılarından günlük enfeksiyon sayılarına ulaşmak için yeni bir model geliştirilmiştir. Elde edilen sonuçlara göre günlük vaka sayısının gerçek bir haftalık döngüye sahip olduğu tespit edildi. Bu haftalık döngüde hesaplanan günlük enfeksiyon sayılarının hafta içi günlerde minimum olduğu saptandı. Bu haftalık minimumların insan gelişmişlik endeksi ve kişi başına düşen yıllık milli gelir gibi sosyo-ekonomik faktörler tarafından kontrol edildiği analiz edilmiştir. Pandeminin yükseliş ve azalış aşamalarında haftalık minimum süre pazartesiden cumaya kayıyor ve virüsün insanlar arasında bulaşması için çalışma ortamı ve sosyal ortam olmak üzere iki ayrı ortam oluşuyor. Üstelik veriler sabit bir üreme sayısından ziyade bir değişkeni ortaya koyuyor. Sonuç olarak bu çalışmada geliştirdiğimiz model, literatürde ilk kez pandeminin ilerlemesindeki sosyo-ekonomik faktörleri enfeksiyon zamanını dikkate alarak başarıyla tespit etmiş ve gelecekteki olası pandemiler için ışık olma potansiyeline sahiptir.

Anahtar Kelimeler: SARS-CoV-2, COVID-19, Enfeksiyon zamanı ve sayısı, Haftalık Döngü.

Acknowledgements

First of all, I would like to thank all my instructors at Abdullah Gül University, Faculty of Life and Natural Sciences and Department of Bioengineering, who contributed to my undergraduate and graduate education, for all their contributions and encouragements.

I express my sincere gratitude to my mentor, Assistant Professor Dr. Altan ERCAN, whom I have been proud to be a student of for four years. I am deeply grateful to him for consistently being a source of inspiration, cultivating my intellectual thinking, contributing significantly to my development through his experiences, as well as through the techniques and thought system he imparted. I extend my gratitude for his unwavering patience, support, and kindness in the laboratory's WET-lab phase and throughout my thesis work.

I wish to extend my heartfelt appreciation to the members of my laboratory. In particular, I would like to express my profound gratitude to Merve SARITAŞ, Zeynep ARICAN, and Gizem Özlem ÖCAL for their invaluable assistance, unwavering support, and motivational guidance during the entirety of this process.

I am deeply grateful to my family, whose unwavering support has been a constant pillar throughout my journey. Their unwavering encouragement has been a driving force behind my endeavors, compelling me to strive for excellence and honor them. My heartfelt thanks extend to my father, Çetin YAĞMUR, whose unwavering support has been invaluable, to my mother, Süreyya YAĞMUR, whose constant well wishes have been a source of strength, to my sister, Zeynep Sude YAĞMUR, who has been a constant wellspring of joy, and to my brother, Muhammed Yasir YAĞMUR, who has been both a guiding figure and a cherished companion.

Additionally, I would like to thank my thesis committee members, Prof. Dr. Ahmet ÖZTÜRK and Doç. Dr. Aysun ADAN, for their support, time, and valuable feedback.

Finally, I thank every organization who contributed to the preparation of this thesis.

TABLE OF CONTENTS

LIST OF FIGURES

LIST OF TABLES

LIST OF ABBREVIATIONS

BTrac	Back Track Method
CDC	Centers for Disease Control and Prevention
CoV	Coronaviruses
COVID-19	Coronavirus Disease 2019
D_{id}	Daily COVID-19 positive cases
I_{nt}	Daily total number of infections
GDP	Gross Domestic Product
HDI	Human Development Index
I_{cd}	Infection on the Current Day
MERS	Middle East Respiratory Syndrome
nCoV	New Coronavirus
NPI	Non-Pharmaceutical Interventions
R_0	Reproductive Number
R_{0i}	Reproductive Number for infection
RNA	Ribonucleic Acid
SARS	Severe Acute Respiratory Syndrome
SARS-CoV-2	Severe Acute Respiratory Syndrome Coronavirus 2
$ssRNA^+$	Single-stranded and positive-sense ribonucleic acid
I_t	Total Infected
UNDP	United Nations Development Program
US	United States
$VarR_0$	Variable Reproductive Number
$VarR_{0i}$	Variable Reproductive Number for infection
WC	Weekly Cycle
WHO	World Health Organization

Chapter 1

INTRODUCTION

1.1 Coronaviruses

Coronaviruses (CoV) are categorized in the group of RNA viruses according to their nucleic acids. They contain single-stranded positive-sense ribonucleic acid ($ssRNA^{+}$) and are also enveloped viruses [1]. Characteristically, they appear as a crown under the electron microscope and corona means crown in Latin. The ultrastructural morphology of the coronavirus is shown in Figure 1.1.1. The reason why it looks crown-shaped is the presence of club-shaped surface glycoprotein projections on its surface [2].

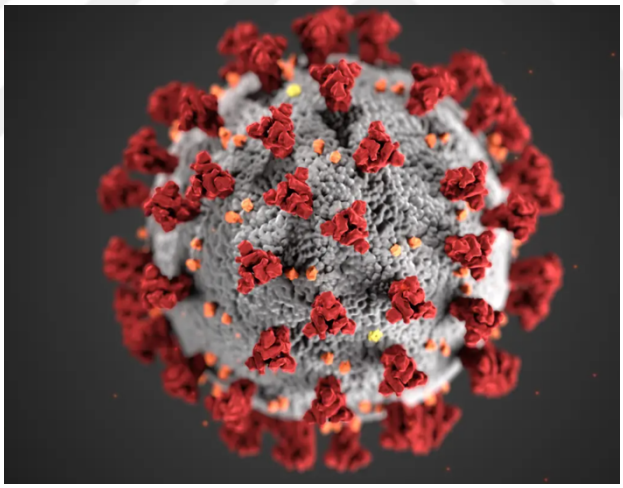

Figure 1.1.1: Illustration of ultrastructural morphology of coronaviruses by Centers for Disease Control and Prevention (CDC). This figure adapted from: [3].

Coronaviruses historically spread widely among mammals and birds, and cause respiratory and intestinal-based diseases but very rarely in humans [4]. It can also cause hepatitis and neurological diseases in some cases [5]. Coronavirus infection appears to be both acute and chronic and has been found to infect its hosts in a species-specific manner. Their species-specific nature arises from the virus's ability to interact with specific cell receptors in a host species, determining its infectivity and adaptation to different animals or humans [4].

The most important distinguishing feature of coronaviruses is that they have the largest genomes and large coding capacity among all RNA viruses [4].

1.2 Classification

Coronavirus was first recognized in the 1960s with the discovery of a few new human respiratory pathogens that appeared to be similar to the previously identified avian infectious bronchitis virus and mouse hepatitis virus [6].

The Coronaviridae family belongs to the order Nidovirales which also includes Arteriviridae, Mesoniviridae, and Roniviridae. Coronaviruses are the largest group of viruses of this order [7]. The common feature of all viruses in the Nidovirales order is that they are unsegmented, enveloped and positive sense RNA viruses. These viruses have large genomes compared to the other RNA viruses, containing approximately 33.5 kb of genome [1]. Another important common feature of the Nidovirales order is their highly conserved genomic organization. They have a large replicase gene preceding structural and accessory genes. Differences within the Nidovirales order occur depending on the type, number and size of structural proteins. As a result of these differences, the morphology of the virus changes significantly [8].

RNA group viruses are divided into 3 groups: Nidovirales, Picornavirales and Tymovirales (Figure 1.2.1). The Nidovirales order, which includes the coronavirus, is divided into 4 families as described above [9]. The Coronaviridae family includes two subfamilies: Coronavirinae and Torovirinae. The Coronavirinae subfamily includes 4 genera: Alphacoronaviruses, Betacoronaviruses, Gammacoronaviruses, and Deltacoronaviruses, according to serology and phylogenetic classification (Figure 1.2.1) [10].

The detailed classification of the coronavirus (SaRS CoV-2) that causes severe acute respiratory syndrome is shown in figure 1.2.1.

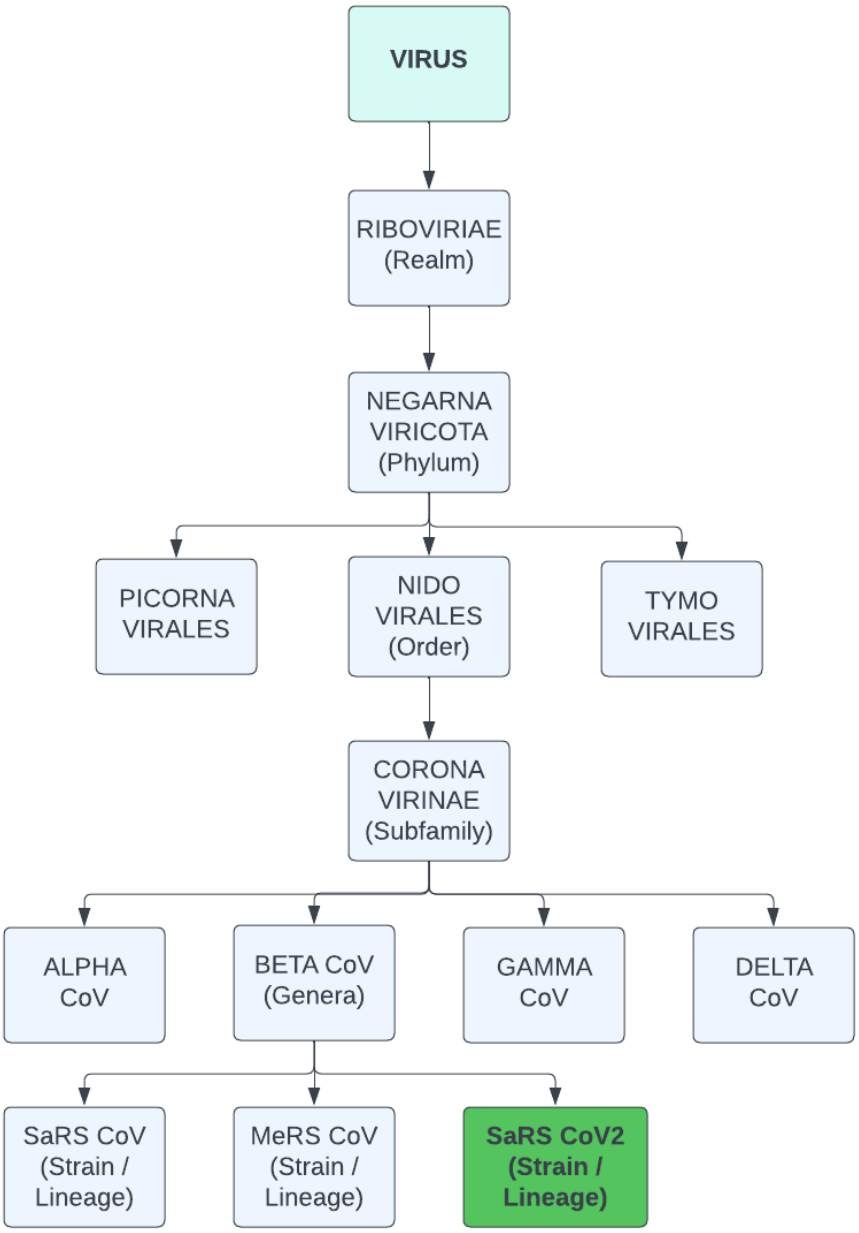

Figure 1.2.1: The schematic representation of the classification and the origin of SARS CoV-2 [1].

1.3 History of Coronavirus

Coronavirus was first identified as a new respiratory tract virus in 1962, in the samples from patients who presented symptoms and complaints of respiratory tract infection [11]. The genomes of the first discovered coronaviruses were generally smaller, approximately 27-32 kilobase pairs (kb), but the genome of SARS-CoV-2 consists of approximately 30 kilobase pairs. Another difference is genetic difference. The genome of SARS-CoV-2 is quite different from other coronaviruses. In particular, it has a

structural protein called spike protein, which is markedly different from that of other coronaviruses[12].

In November 2002, the first case of SARS infection appeared in Guangdong province in China. According to WHO, 305 people were infected and 5 people died. This was the first official report for the SARS epidemic by WHO. An interesting point in this report is that nearly 30% of the cases were healthcare personnel involved in patient care [13]. In addition, the first cases of the epidemic occurred among people working in food establishments of animal origin. A total of 24 countries were affected by SARS virus, which started in November 2002 and continued for a while, in Cambodia, Hong Kong, Singapore, Hanoi and Canada. In total, approximately 8,500 SARS-CoV cases and 813 deaths were reported [14].

MERS (Middle East Respiratory Syndrome) is a disease caused by the virus called MERS-CoV, which belongs to the coronavirus family and emerged in Saudi Arabia in 2012, causing serious respiratory diseases. MERS is generally transmitted to humans from dromedary camels, with limited transmission potential between humans. MERS has been observed to cause serious complications such as acute respiratory failure and kidney failure[15].

In December 2019, a significant escalation in the incidence of acute respiratory distress, marked by the manifestation of symptoms akin to pneumonia, identified within the urban areas of Wuhan, the capital city of Hubei province in the People's Republic of China. It was subsequently reported that this group of patients was infected with a new coronavirus (nCoV) that has never been seen to infect humans before [16]. This new virus, which has a similar symptom to SARS, was first called as "nCoV 2019". Later, the World Health Organization and the China Bureau reported this virus, a new coronavirus called COVID-19 and disease it causes as Severe Acute Respiratory Syndrome Coronavirus 2 (SARS-CoV-2) The discovery of this new coronavirus was made by isolating it from individuals with pneumonia [17].

It has been determined that COVID-19 infects people more efficiently than SARS and MERS viruses, which caused epidemics in 2002 and 2012, respectively [18]. Another factor as effective as genetic factors in the rapid spread of this virus all over the world is that it spread from Wuhan, an important transportation center of China and a crowded province where 11 million people live [17].

As of October 15, 2023, WHO documented a total of 771 million confirmed cases of SARS-CoV-2, along with 6.9 million fatalities on a global scale.

1.4 Global Spread of COVID-19 and Health Crisis

The insightful and prescient perspective, as illuminated by the pioneering research of Kermack and McKendrick in 1927, highlights the interconnected nature of population growth with the increased likelihood of infectious disease outbreaks [19]. This underscores the ongoing challenge posed by such situations in modern society. In short, it is not a realistic perspective to imagine living without epidemics and pandemics in the future.

Towards the end of 2019, an unidentified illness surfaced in Wuhan, China, characterized by symptoms related to upper respiratory tract infections. In a relatively brief period thereafter, the origin of this disease was traced back to a virus named as COVID-19 and the disease named as the SARS-CoV-2, a designation conferred by the WHO [20]. Unfortunately, the COVID-19 virus has spread at a speed never seen before and first became an epidemic and then a pandemic in the world [21].

The fact that this strain of Coronavirus has a very high transmission capacity which allowed it to turn into a global pandemic all over the world. This caused the collapse of healthcare systems around the world, surprising governments and almost rendering them unable to act. It is obvious that there was an imperative need to take urgent and effective measures to manage this epidemic to reduce its effects [21].

1.5 The Initial Response to the COVID-19 Pandemic

The first interventions to the COVID-19 pandemic, which had a great impact in the world, included the implementation of various non-pharmaceutical interventions (NPIs) to prevent the transmission of the virus [22]. This included information explaining the benefits of using face masks, personal hygiene and frequent hand/face washing. In addition, the concept of social distancing was explained to the public. According to the status of the pandemic, harsher and stricter interventions than those were imposed such as staying at home and restrictions on working hours. All of these non-pharmaceutical interventions varied from country to country and over time [23].

Differences in the implementation of NPIs can be exemplified by the different implementation by different states in the United States. While NPIs in some states were followed early and strictly, the situation in some states was the opposite. Of course, this

has caused differences in the spread of the virus and the number of cases between these states [24].

Similarly, important findings were found in the study conducted in Germany on the change of reproduction number (R_0) in the number of SARS-CoV-2 cases. The timing of the measures determined by the political authorities in this country and the frequency of these measures have caused the change in the number of daily case numbers. The importance of the time and frequency of these measures for the health system was clearly revealed [25].

The initial measures included staying at home and restricting working hours and extended to travel restrictions. A study conducted in China revealed that travel bans, and stay-at-home measures were very important in controlling the virus, but it wasn't enough to stop the spread of the virus. Therefore, much more strict measures in China were implemented intensively, literally shutting down cities and regions in order to prevent the rapid spread of the virus. This meant strict curfews and quarantines. In particular, the city of Wuhan was considered to be the center of the pandemic, so a complete lockdown was implemented and people's movements in and out of the city were limited. The implementation of these radical measures helped to bring the epidemic under control quickly. These NPIs resulted in the considerable decrease in new daily case numbers, easing high pressure on the healthcare system. However, such strict measures also brought out economic and social difficulties. For example, business closures and curfews have seriously affected the daily lives of many people. At this point, the development of the countries in different areas such as education and Gross domestic product (GDP) are seen as important points [26].

In conclusion, the response to the SARS-CoV-2 pandemic involved a variety of NPIs, from personal hygiene recommendations to more drastic measures depending on the evolving understanding of how the virus spread and the specific precautions according to the perspectives by each country or region. These interventions have clearly played an important role in mitigating the impact of the epidemic and continued to be adapted to the evolving nature of the crisis [27].

1.6 Concept of Herd Immunity and Lessons from COVID-19 Pandemics

Understanding and achieving herd immunity against a pathogen like COVID-19 virus is a critical aspect in managing its transmission within a population. Traditionally, this immunity is established by either exposing individuals to a milder strain of the pathogen or more commonly through widespread vaccination efforts, particularly in the case of COVID-19 virus [28].

Vaccination of a large proportion of populations is necessary to achieve herd immunity to reduce COVID-19 transmission and save vulnerable individuals from the severe effects of the disease. Herd immunity requires a 75-85% vaccination rate in the population. Additionally, as the intensity of the infection increases, the number of individuals who need to be vaccinated also increases [28]. Another study estimated that 83% of the population needed to become immune to reach the herd immunity threshold [29]. However, at this point, the fair distribution of the vaccine, people's acceptance of vaccination and the unknown response of the new variants of the virus towards the vaccine were among the difficulties in the effort to achieve herd immunity.

Effective collaboration of different institutions in the fight against the pandemic, such as researchers, health experts and policy makers, is also very important for the future of the pandemic and its impact on society. The joint and harmonious effort for vaccination campaigns put forward to reach a successful herd immunity. However, the vaccination campaigns didn’t result in reaching the expected level for lowering the daily case numbers while lowering the daily death number [30]. This experience shows that vaccination may not be enough to lower the daily case numbers and points to need for the alternatives based on the mechanism of virus probation.

1.7 Effect of vaccination

To begin, it has become evident that the swift global propagation of this virus with four million daily cases recorded worldwide from December 21, 2021, to April 30, 2022, constitutes a significant public health challenge. Conducting research to reveal the most important factors affecting the transmission of the COVID-19 virus can offer significant perspectives on limiting the virus transmission [30]. The high contagiousness of the COVID-19 virus is the main factor that causes rapid spread. It may be possible for the infectious rate to increase further as a result of the evolution of different variants of this virus [30-32] .

One of the most important factors in preventing the spread of the virus is a successful vaccine and vaccination process. The development of vaccines with an effectiveness of up to 95% is one of the important achievements [33, 34]. The availability of multiple vaccines, especially those from Novavax, BioNTech and Moderna, has supported the effort to protect populations against the virus. Highly effective vaccines have been proven in slowing the spread of the virus and reducing the impact of the pandemic [35, 36].

In summary, the rapid transmission of COVID-19 virus and the production of the effective vaccines helped to control rapid spread of the virus between 21 December 2021 and 30 April 2022. In order to control such epidemics that affected the whole world, scientific research was of great importance due to a good understanding of the characteristics of the virus and the development of effective vaccines. This pandemic process has taught valuable lessons on ways to protect public health and limit the growth of the pandemic's impact.

Despite comprehensive restrictions and global vaccination campaigns, the SARS-CoV-2 pandemic continued to affect life in 2023. The distinctive nature of the COVID-19 virus and the different variants it has evolved and have made the pandemic difficult to manage and control.

1.8 Mutations and Variants of COVID-19 Virus

The COVID-19 virus possesses a single-stranded positive sense RNA. Its mutation rate is relatively low at approximately $1.3 \times 10^{-6} \pm 0.2 \times 10^{-6}$ per cycle [37]. Despite this, its efficiency in spreading during the pandemic wasn't fully impeded due to its high replication rate, infectivity rates and large number of naive populations. The virus undergoes rapid evolution leading to the emergence of new variants within a short timeframe [38].

Mutations in the virus have led to the emergence of new variants with faster replication rates and transmission characteristics, especially alpha, beta, gamma and delta variants resulting in the diversification of existent variants [37, 39].

The formulation and modification of the pandemic management plans, vaccination programs, and the public health policies are greatly aided by this information, which also highlights crucial and intricate problems that require constant surveillance. At the end, the mutation rates of COVID-19 virus are what causes the fast spread of many variations,

including the development of specific variants like alpha, beta, gamma, and delta. This demonstrates the growing significance of gaining a better comprehension of evolutionary dynamics of the virus and the population's alterations.

The emergence of new variants has demonstrated their capacity to re-infect individuals who have recovered from COVID-19 virus infection or have been vaccinated against previous variants [40]. This highlights that acquired immunity might not offer expected protection against new strains like the BQ and XBB subvariants of Omicron [41]. Despite this, world-wide vaccination efforts have shown success in reducing hospitalization and mortality rates [42]. Although the limitations of existing NPIs and vaccines have become evident [43], it is clear that they are not enough to stop the pandemics and therefore there is an urgent need to design alternative approaches to effectively manage the spread of the virus.

Therefore, to control the spread of COVID-19, alternative approaches need to be developed alongside NPIs and vaccines. Relying solely on existing vaccines and NPIs is not sufficient, because as new variants develop and immune memory becomes ineffective, there is an increasing need to study additional treatment and protection strategies. Scientists are constantly striving to develop rapid and effective responses to these new threats. This reflects the need for a continuous learning process and flexibility to manage the pandemic.

1.9 Human Development Index and GINI Index

Human Development Index (HDI) is a term introduced by the United Nations Development Program (UNDP) and accepted as a unit of measurement that evaluates the development of countries from a broad perspective. Its primary objective is to consider not only economic advancement but also the standards of living and overall well-being of a society. HDI serves as a tool for both ranking countries and monitoring their advancement in the realm of human development. There are 3 fundamental indexes in the Human Developmental Index calculation [44]:

1. Life Expectancy at Birth: This component reflects how long a country's population lives on average. Usually, this component is represented by life expectancy (life expectancy).
2. Education: The education component is divided into two subcomponents:

a. Literacy and Basic Education: This component includes basic education indicators such as a country's literacy rate.

b. Average Years of Education of People: This component reflects the average years of education of a country's population.

3. GDP (Gross Domestic Product) - Purchasing Power Parity (Gross Domestic Product - Purchasing Power Parity, GDP-PPP): This component represents the economic well-being of a country and calculates GDP per capita in purchasing power parity. This reflects a country's economic productivity.

When calculating HDI, each component is compressed into a specific range and the results are combined to calculate the HDI value. The HDI value is a number between 0 and 1. 1 represents the highest level of human development while 0 represents the lowest.

HDI is a common tool for evaluating the development levels and differences of countries and helps policymakers in directing development efforts. However, HDI also has its criticisms, because this index is based only on some basic indicators and may not fully reflect all human development. Therefore, a more comprehensive assessment can be made by using other indicators and the HDI data together.

The GINI index was developed by Italian statistician Corrado Gini in 1912. The GINI index, also known as the GINI coefficient, is the most common measure of inequality and is often used as a measure of income inequality [45].

The GINI index offers the benefit of summarizing the overall income distribution inequality through a single statistic that is straightforward to interpret, ranging between 0 and 1.

It is stated that as values increase, inequality increases, while when values decrease, inequality decreases. That is, a value of 0 represents perfect equality, where everyone in that society has the same value. On the other hand, a value of 1 indicates that one person receives all income and the rest receive no income [45].

1.10 The Weekly Cycle of Daily Case Number and Its Possible Origin

It is obvious that it is necessary to develop more effective methods to prevent the transmission of the COVID-19 virus. The primary mechanism of virus spread is when an infected individual and a vulnerable individual interact with each other in close proximity in a shared time and space which potentially can lead to new infections [46].

The daily diagnosis numbers (D_{id}) for most countries peak on weekdays (Monday to Friday) and dipped on weekends (Saturday and Sunday) [47]. This pattern was also visible in the number of daily tests performed with a peak during the weekdays and a bottom on the weekends at the relatively early days of the pandemic [48, 49]. For example, strong linear correlation coefficients between these variables were found in New York City, NY, and Los Angeles, CA, with R^2 values of 0.96 and 0.83, respectively [49]. Consequently, a weekly cycle (WC) in D_{id} was initially deemed as an outcome of the daily applied COVID-19 tests and discrepancies in reporting between weekdays and weekends at the pandemic's onset [49]. Subsequently, it was inferred that the WC of D_{id} is an artifact of the daily tests administered.

In this study, the relationship between WC and the number of tests was examined and it was aimed to understand whether the above conclusion is correct or not. With this understanding, a Backtracking (BTrac) method was developed to calculate the total daily number of infections (I_{nt}), implemented using D_{id} data. Unlike D_{id}, I_{nt} shows a low level on a weekly basis during the week, which is affected by socio-economic factors such as GDP per capita income, HDI and national holidays. Additionally, the reproductive number (R_0), which represents the average number of secondary infections caused by an individual per day, was calculated by dividing I_{nt} by the previous day's value and exhibits a similar WC pattern as D_{id} and I_{nt} in real-world data. This discovery was combined with the previous method to form the Variable R_0 value of infection ($VarR_{0i}$) method. This new method can help us better understand the mechanism of virus spread and predict the changes in the course and the spread of infections based on real-world data.

The $VarR_{0i}$ approach effectively mirrors the WC observed in real-world data, predicting a 50% reduction in infections if the infectivity of the virus decreases by 11% in the second half of seven consecutive weeks. By tracking and predicting changes in the rate of spread of the virus based on real-world data, this approach suggests that infections could be decreased significantly once there is a certain downward trend. This may actually offer a specific road map in controlling the virus and reducing the number of infections.

Here in this study, it is proved that weekly cycle (WC) of D_{id} is not an artifact. Based on this hypothesis, a Back Tracing (BTrac) method is developed to calculate I_{nt} from D_{id}. The calculated I_{nt} has WC as in D_{id} but unlike D_{id}, WC of I_{nt} has a weekly minimum during the weekdays and is controlled by the socio-economic factors such as the Gross

Domestic Product per capita, Human Development Index and national holidays. In addition, R_{0i}, which is defined here as the number of secondary infections caused by an infected individual per day in average and calculated by dividing I_{nt} by the same value for the day before, exhibits WC as in the case of D_{id} and I_{nt} for real world data. Combining this observation with the above method gives rise to a Variable R_{0i} ($VarR_{0i}$) method.

In this context, it is imperative to emphasize that the observed weekly cycle (WC) of D_{id}, originally considered an artifact, bears significant implications for our understanding of the COVID-19 spread and pandemic dynamics. This research demonstrates that WC of D_{id} is not a mere artifact, but rather a manifestation of intricate transmission patterns intertwined with numerous socio-economic variables. Consequently, we have developed a novel analytical framework, the Back Tracing (BTrac) method, to derive the daily total number of infections (I_{nt}) from D_{id}. Notably, our findings reveal that I_{nt} also exhibits a discernible weekly cycle, distinguished weekdays. This compelling insight underscores the significant influence of socio-economic factors, including GDP per capita, HDI, and national holidays, on the weekly fluctuations observed in D_{id} and I_{nt}.

Moreover, this study introduces a critical epidemiological metric, representing the average number of secondary infections attributed to an individual per day. It is computed by dividing I_{nt} for a given day by the corresponding value for the previous day. Strikingly, R_0 exhibits a WC pattern mirroring that observed in D_{id} and I_{nt} when applied to real-world data. Building on this observation, we introduce a novel approach, the $VarR_{0i}$ method, which replicates the WC pattern evident in real-world data. As it indicated, our $VarR_{0i}$ approach proves invaluable for predictive modeling, illustrating that a modest 11% reduction in virus transmission over the latter half of seven consecutive weeks could lead to a 50% decrease in projected infections.

These findings underscore the vital role of detailed transmission dynamics, socio-economic variables, and predictive models in the ongoing global effort to comprehend and mitigate the COVID-19 pandemic. By offering a refined understanding of the weekly fluctuations in COVID-19 diagnoses and infections, our research contributes to the development of more effective strategies for pandemic management, rooted in evidence-based insights into the multifaceted factors at play in this global health crisis.

Chapter 2

Material and Methods

2.1 The online data sources:

The data utilized in this analysis has been acquired from publicly available online platforms. The dataset concerning the correlation between daily COVID-19 positive cases and test numbers was acquired from the Our World In Data website (www.ourworldindata.org). Additionally, for a more extensive examination encompassing 46 countries, the daily case number data was accessed from https://data.humdata.org/dataset/coronavirus-covid-19-casesand-deaths . Socio-economic factors such as GDP, GDP per capita, GINI index, and HDI were gathered from reputable sources including the World Bank website (https://data.worldbank.org/indicators) for GDP-related data and the World Population Review website (https://worldpopulationreview.com/countries) for HDI information.

2.2 Determining the relation between the daily case and test numbers using linear regression analysis

The dataset pertaining to the temporal correlation between D_{id} and daily test numbers was retrieved from www.ourworldindata.org. To ensure consistency and reliability, a meticulous examination was conducted on continuous D_{id} and test numbers spanning from March 2020 to January 2021, considering countries with populations exceeding four million and reliable continuous data of test and diagnosis numbers. Out of these considerations, 23 countries were selected (refer to Table 2.2.1 for the comprehensive list of countries and associated dates) due to the limited available data.

Table 2.2.1 The list of the countries and time intervals for the linear correlation between daily diagnosis and the daily test numbers

Name of the country	The dates and related R^2 values
1. Argentine	Initial phase from 03/03/2020 to 18/05/2020 Middle phase from 19/05/2020 to 08/08/2020 Late phase from 09/08/2020 to 12/01/2021
2. Bolivia	Initial phase from 15/03/2020 to 15/05/2020 Middle phase from 16/05/2020 to 04/08/2020 Late phase from 05/08/2020 to 14/01/2021
3. Bulgaria	Initial phase from 02/05/2020 to 09/06/2020 Middle phase from 10/06/2020 to 17/08/2020 Late phase from 18/08/2020 to 17/01/2021
4. Chile	Initial phase from 10/04/2020 to 12/07/2020 Middle phase from 13/07/2020 to 13/09/2020 Late phase from 14/09/2020 to 17/01/2021
5. Colombia	Initial phase from 06/06/2020 to 06/08/2020 Middle phase from 07/08/2020 to 15/09/2020 Late phase from 16/09/2020 to 17/01/2021
6. Denmark	Initial phase from 08/03/2020 to 09/04/2020 Middle phase from 10/04/2020 to 12/09/2020 Late phase from 13/09/2020 to 14/01/2021
7. France	Phase-Initial from 13/05/2020 to 17/07/2020 Middle phase from 18/07/2020 to 11/09/2020 Phase-late from 12/09/2020 to 14/01/2021
8. Greece	Phase-Initial from 13/03/2020 to 28/07/2020 Middle phase from 29/07/2020 to 21/09/2020 Late phase from 22/09/2020 to 2021-01-17/01/2021
9. Guatemala	Phase-Initial from 19/03/2020 to 07/05/2020 Middle phase from 08/05/2020 to 14/06/2020 Phase-late from 15/06/2020 to 15/01/2021
10. Hungary	Phase-Initial from 13/03/2020 to 01/09/2020

	Middle phase from 02/09/2020 to 13/10/2020 Phase-late from 14/10/2020 to 17/01/2021
11. Israel	Phase-Initial from 05/03/2020 to 01/06/2020 Middle phase from 2020-06-02 to 15/11/2020 Phase-late from 16/11/2020 to 11/01/2021
12. Italy	Phase-Initial from 25/02/2020 to 25/03/2020 Phase-Middle from 26/03/2020 to 06/10/2020 Phase-Late from 07/10/2020 to 17/01/2021
13. Kazakhstan	Phase-Initial from 14/03/2020 to 17/05/2020 Middle phase from 18/05/2020 to 01/07/2020 Phase-Late from 02/08/2020 to 13/01/2021
14. Mexico	Initial phase from 28/02/2020 to 22/04/2020 Middle phase from23/04/2020 to 16/06/2020 Late phase from 17/06/2020 to 16/01/2021
15. Morocco	Initial phase from 16/03/2020 to 23/07/2020 Middle phase from 24/07/2020 to 18/10/2020 Late phase from 19/10/2020 to 15/01/2021
16. Nepal	Phase-Initial from 11/03/2020 to 03/06/2020 Middle phase from 04/06/2020 to 30/09/2020 Late phase from 01/10/2020 to 15/01/2021
17. Poland	Initial phase from 29/04/2020 to 22/05/2020 Middle phase from 23/05/2020 to 17/09/2020 Late phase from 18/09/2020 to 16/01/2021
18. Portugal	Initial phase from 4/3/2020 to 6/4/2020 Middle phase from 7/4/2020 to 8/9/2020 Late phase from 9/9/2020 to 13/01/2021
19. Romania	Initial phase from 13/03/2020 to 10/04/2020 Middle phase from 11/04/2020 to 07/10/2020 Later phase from 01/10/2020 to 10/01/2021
20. Serbia	Initial phase from 10/03/2020 to 15/04/2020 Middle phase from 16/04/2020 to 25/10/2020 Late phase from 26/10/2020 to 17/01/2021
21. SouthAfrica	Initial phase from 12/03/2020 to 07/05/2020 Middle phase from 08/05/2020 to 19/08/2020

	Later phase from 20/08/2020 to 17/0/2021
22. UnitedKingdom	Phase-Initial from 31/03/2020 to 11/07/2020 Middle phase from 12/07/2020 to 24/09/2020 Late phase from 25/09/2020 to 14/01/2021
23. US	Initial phase from 01/03/2020 to 31/03/2020 Middle phase from 01/04/2020 to 20/10/2020 Late phase from 21/10/2020 to 12/01/2021

Due to the inherent disparities within the data, stemming from factors like varying test supply logistics and reporting inconsistencies, particularly during the initial stages of the pandemic, a three-phase analysis was undertaken. The dates for these phases are adjusted so that to give the best possible three linear relations between the daily test and diagnosis numbers. These phases—initial, middle, and late—are aimed at establishing the most optimal linear correlation trends between Did and daily test numbers through non-linear regression analysis (expressed as y = y0 + a Did, where y represents the daily test number and a is a constant). For example, the outcomes revealed differing linear correlation coefficients for the United States: 0.900 for the period from 1st to 31st March 2020, 0.556 for 1st April to 20th October 2020, and 0.225 for 21st October 2020 to 12th January 2021 (refer to Fig. 3.1.1 – 3.1.2 for graphical representations).

2.3 Development of a model to backtrack the time of infection from the daily number of diagnosis

The transmission dynamics of the COVID-19 virus follow a distinct sequence: initial exposure of a susceptible individual to the virus, an incubation period, and subsequent diagnosis of the infected individual. In the case of COVID-19, the minimum incubation period is estimated to be 3 days with diagnosis typically occurring around the 6 day post-infection and possibly extending up to 14 days after exposure to COVID-19 virus [50, 51]. These estimations are derived from various methodologies, including contact tracing, filiation studies, and mathematical models. Additionally, the distribution of the day of diagnosis conforms to a Weibull distribution [52]. By utilizing above parameters these parameters, a novel method has been developed in this context.

This novel approach involves retroactively determining infection time by COVID-19 virus using Rayleigh distribution, a special case of Weibull distribution (with k = 2 and L = 0.5) (Fig. 2.3.1). Aligning the peak of the Rayleigh distribution with the average peak of D_{id}, it covers a lag of 3 to 14 days.

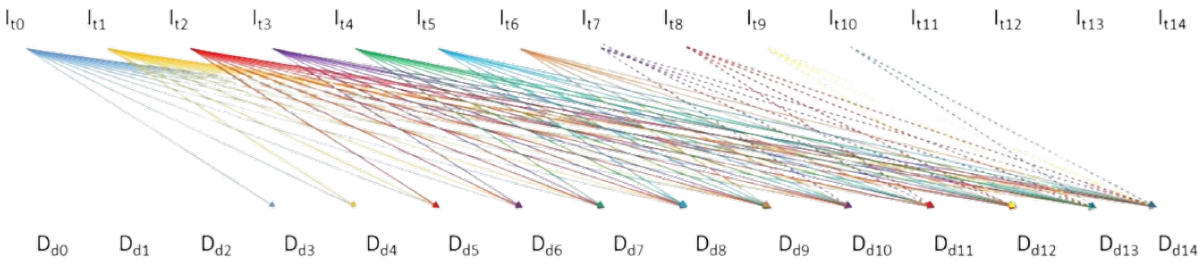

Figure 2.3.1 The conversion of the daily diagnosis number to daily infection number by BTrac and its time dependent variation. The contribution of I_{nt} to D_{id} for the next 14 days is presented with different colors.

The equation $I_{cd} = D_{i\,d}\, k\, L^{\,k}\, d^{\,k-1}\, e^{\,-(l\,d)\,\wedge k}$ computes daily contributions to total diagnoses over 14 days from the day of infection (Fig. 3.2.1). Utilizing this equation, past 14-day D_{id} distribution is calculated, and daily total I_{nt} numbers are derived by summing I_{cd} contributions (Fig. 3.2.1). This method is applied to data for 46 countries (refer to Table 2.3.1) with populations of four million or more, containing consistent daily new case data sourced from the official United Nations webpage (https://data.humdata.org/dataset/coronavirus-covid-19-cases-and-deaths) without any anomalies in their time-dependent continuity.

Table 2.3.1 The list of 46 countries, related dates for the increasing and decreasing phases of the COVID 19 pandemic.

	Peak 1		Peak 2		Peak 3	
	Increasing Phase	Decreasing Phase	Increasing Phase	Decreasing Phase	Increasing Phase	Decrease Phase
Argentina	21/9/2020	26/10/2020	26/4/2021	31/5/2021	20/12/2021	24/1/2022
Armenia	21/9/2020	9/11/2020	22/2/2021	12/4/2021	13/9/2021	1/11/2021
Austria	12/10/2020	23/11/2020	15/2/2021	29/3/2021	25/10/2021	29/11/2021
Azerbaijan	9/11/2020	14/12/2020	15/3/2021	19/4/2021	2/8/2021	6/9/2021
Bangladesh	25/5/2020	13/7/2020	1/3/2021	19/4/2021	20/12/2021	7/2/2022
Belarus	20/4/2020	1/6/2020	16/11/2020	28/12/2020	20/9/2021	1/11/2021
Brazil	29/6/2020	3/8/2020	15/2/2021	29/3/2021	3/1/2022	7/2/2022
Bulgaria	12/10/2020	30/11/2020	1/3/2021	5/4/2021	27/9/2021	8/11/2021
Canada	30/11/2020	11/1/2021	15/3/2021	19/4/2021	6/12/2021	17/1/2022
Chile	11/5/2020	22/6/2020	8/3/2021	19/4/2021	3/1/2022	21/2/2022
Colombia	20/7/2020	24/8/2020	21/12/2020	25/1/2021	24/5/2021	5/7/2021
Croatia	2/11/2020	21/12/2020	8/3/2021	26/4/2021	27/9/2021	15/11/2021
Czechia	21/9/2020	9/11/2020	1/2/2021	22/3/2021	27/12/2021	14/2/2022
Dominican Republic	22/6/2020	3/8/2020	14/12/2020	25/1/2021	3/5/2021	14/6/2021
Egypt	18/5/2020	29/6/2020	30/11/2020	4/1/2021	12/4/2021	24/5/2021
France	5/10/2020	9/11/2020	8/3/2021	19/4/2021	20/12/2021	31/1/2022
Germany	16/11/2020	28/12/2020	15/3/2021	26/4/2021	25/10/2021	6/12/2021
Greece	5/10/2020	23/11/2020	8/3/2021	19/4/2021	6/12/2021	17/1/2022
Guatemala	15/6/2020	27/7/2020	19/7/2021	6/9/2021	10/1/2022	21/2/2022
Hungary	19/10/2020	7/12/2020	22/2/2021	5/4/2021	25/10/2021	6/12/2021
India	10/8/2020	28/9/2020	5/4/2021	17/5/2021	20/12/2021	31/1/2022
Indonesia	21/12/2020	8/2/2021	14/6/2021	26/7/2021	17/1/2022	21/2/2022
Iraq	3/8/2020	21/9/2020	15/3/2021	3/5/2021	21/6/2021	9/8/2021
Iran	26/10/2020	7/12/2020	15/3/2021	3/5/2021	12/7/2021	30/8/2021
Israel	24/8/2020	12/10/2020	7/12/2020	25/1/2021	26/7/2021	13/9/2021
Italy	5/10/2020	23/11/2020	8/2/2021	29/3/2021	6/12/2021	17/1/2022
Japan	7/12/2020	18/1/2021	12/7/2021	30/8/2021	3/1/2022	21/2/2022
Kazakhstan	15/3/2021	3/5/2021	14/6/2021	2/8/2021	13/12/2021	31/1/2022
Lebanon	14/12/2020	25/1/2021	5/7/2021	23/8/2021	27/12/2021	14/2/2022
Mexico	14/12/2020	25/1/2021	12/7/2021	30/8/2021	13/12/2021	31/1/2022
Morocco	5/10/2020	23/11/2020	28/6/2021	16/8/2021	13/12/2021	31/1/2022
Nigeria	25/5/2020	13/7/2020	14/12/2020	1/2/2021	12/7/2021	30/8/2021
Norway	7/9/2020	26/10/2020	15/2/2021	5/4/2021	3/1/2022	21/2/2022
Pakistan	4/5/2020	22/6/2020	26/10/2020	14/12/2020	15/3/2021	3/5/2021
Poland	5/10/2020	23/11/2020	22/2/2021	5/4/2021	25/10/2021	13/12/2021
Portugal	12/10/2020	23/11/2020	21/12/2020	8/2/2021	27/12/2021	7/2/2022
Romania	12/10/2020	30/11/2020	15/2/2021	5/4/2021	13/9/2021	1/11/2021
Russia	16/11/2020	4/1/2021	7/6/2021	26/7/2021	27/9/2021	15/11/2021
Saudi Arabia	11/5/2020	29/6/2020	24/5/2021	12/7/2021	13/12/2021	31/1/2022
Serbia	26/10/2020	14/12/2020	22/2/2021	12/4/2021	23/8/2021	11/10/2021
South Africa	8/6/2020	27/7/2020	30/11/2020	18/1/2021	24/5/2021	12/7/2021
Spain	21/12/2020	8/2/2021	14/6/2021	9/8/2021	13/12/2021	7/2/2022

Turkey	9/11/2020	28/12/2020	8/3/2021	26/4/2021	27/12/2021	14/2/2022
United Arab Emirates	13/4/2020	1/6/2020	21/12/2020	8/2/2021	6/12/2021	24/1/2022
United Kingdom	30/11/2020	18/1/2021	7/6/2021	26/7/2021	6/12/2021	17/1/2022
United States	30/11/2020	18/1/2021	2/8/2021	20/9/2021	6/12/2021	24/1/2022

2.4 Weekly Minimum Graphs and Simulation Model using Var_{0i}

Here's a breakdown of the process involved in the $VarR_0$ model:

1. Calculation of I_{cd} (Infection on the Current Day):

   Multiply the I_{nt} value with the R_0 value for the following day to obtain the I_{cd} value.

2. Distribution of I_{cd} for Future Days:

   Distribute this I_{cd} value for the next 14 days using a Rayleigh distribution to determine the day of diagnosis (D_i).

3. Calculation of D_{id} (Daily Diagnosed Cases):

   Sum up I_{cd} values from the past 14 days following the day of transmission to determine D_{id}.

4. Adjustment of Total Infected but Undiagnosed Population (I_t):

   Subtract D_{id} from the total infected but not diagnosed (I_t) population to calculate It at the end of the day.

Regarding the simulation for $VarR_{0i}$:

The simulation initiates with two weeks of variable high R_{0i} values (0.7, 0.8, 0.9, 1.0, 1.2, 1.3 from Mon to Sun), followed by lower variable R_{0i} values to simulate the onset and progression of the SARS-CoV-2 pandemic.

Additionally, the time interval from infection to diagnosis averages at a maximum of two weeks.

This methodology essentially simulates how infections occur, progress, and are diagnosed over a specified time period, considering variations in R_{0i} values and the time taken for diagnosis.

2.5 Statistical Analysis

Statistical analysis involved the conversion of D_{id} to I_{nt}, as well as the normalization of I_{nt} and simulations incorporating constant and variable R_{0i} values, executed through SigmaPlot for Windows Version 10.0 software. Spearman's r, one-tailed, was employed for assessing correlations among different variables, utilizing GraphPad Prism 4. Additionally, distinctions between two groups were ascertained via the one-tailed Mann-Whitney test in GraphPad Prism 4. Graphs representing the outcomes were generated using GraphPad Prism 4 and SigmaPlot for Windows Version 10.0 software.

After obtaining I_{nt} values, these values were normalized by value on Monday of each week for each of the 46-country using Microsoft Excel 2019 version. Then, 27 charts covering 108 weeks were drawn for each country using the following codes in the Python 3.12.1 programming language (An example Fig. 3.2.2).

```
#from builtins import int
#from mpl_tools import *
import numpy as np
from matplotlib import pyplot as plt
import pandas as pd

sheets = '''Argentina
Austria
Azerbaijan
Bangladesh
Belarus
Bolivia
Brazil
Bulgaria
Canada
Chile
Colombia
Costa Rica
```

Czechia

Denmark

Dominican Republic

Egypt

France

Germany

Greece

Guatemala

Honduras

Hungary

India

Indonesia

Iran

Israel

Italy

Japan

Kazakhstan

Lebanon

Mexico

Morocco

Netherlands

Nigeria

Norway

Pakistan

Peru

Poland

Portugal

Romania

Russia

Saudi Arabia

Serbia

South Africa

Spain

Sweden

```
Turkey
United Arab Emirates
Ukraine
United Kingdom
United States
Hong Kong
Croatia
Armenia
Kuwait
Iraq'''

sheet_done = """

def save_figures(sheet_name, file_dir, excel_dir, start_line, end_line):
    #xls = pd.ExcelFile('IEY.xlsx')
    df = pd.read_excel(excel_dir, sheet_name=sheet_name, engine='openpyxl')


    country = sheet_name



    arr2 = df["Norm Equ"][start_line:end_line]
    date = df["Date"][start_line:end_line]

    xticks = ["Monday", "Tuesday", "Wednesday", "Thursday", "Friday",
"Saturday", "Sunday"]

    for ind, i in enumerate(range(0, len(arr2), 28)):
        month = list(arr2[i:i + 28])
        week1 = month[:7]
        week2 = month[7:14]
        week3 = month[14:21]
        week4 = month[21:]
```

```
            subtitle_string = f'{sheet_name} \n {date[i].strftime("%m/%d/%Y")} -
{date[i + 27].strftime("%m/%d/%Y")}'

            plt.title(subtitle_string, fontsize=10)
            plt.plot(xticks, week1, label="Week 1", linestyle="-", marker='o')
            plt.plot(xticks, week2, label="Week 2", linestyle="-", marker='o')
            plt.plot(xticks, week3, label="Week 3", linestyle="-", marker='o')
            plt.plot(xticks, week4, label="Week 4", linestyle="-", marker='o')
            plt.legend()
            plt.savefig(f'{file_dir}/{sheet_name}_month-{(ind+1)}.png')
            #plt.show()
            plt.clf()


    with open('readme.txt', 'w') as f:
        f.writelines("_____\n")

    for country in sheets.split('\n'):
        print(country)

        save_figures(country.strip(), 'figures', 'XXXnormalized.xlsx', 0, 756)
        #save_figures('Belarus', 'figures')
```

Chapter 3

RESULTS

3.1 WC Is a Part of The Mechanism for Virus Transmission but Not an Artifact of The Daily Test Number

During the onset of the COVID-19 pandemic, a noticeable weekly pattern emerged in the recorded daily case and test numbers. The trend is that the number of cases increases on certain days of the week as in the number of tests performed. Moreover, a strong linear relationship between them was identified [49]. This led to an early conclusion that this correlation resulted from the test numbers, indicating it might be an outcome of testing policies rather than a genuine connection.

The current study is based on the hypothesis that WC is a result of D_{id} rather than by the daily test count. Therefore, this must be an intrinsic nature of virus propagation in general such as COVID-19 virus in specific. In this context, this investigation delves into the cause-and-effect relationship between the daily case and test numbers, utilizing the linear correlation coefficient (R^2) as an indicator. From March 2020 to January 2021, D_{id} and test numbers from 23 countries were selected for investigation across three phases—initial, middle, and late—aiming to identify the best three linear correlation coefficients (R^2) to optimize the each R^2 value and minimize the possible mistakes.

The selection of 23 countries for analysis was based on data availability regarding their daily case and test numbers, considering irregularities and unique characteristics within each country's dataset (see the Table 3.1.1 for the list of countries, phases dates and R^2 values). This spanned from March 2020 to January 2021, aiming for consistency and completeness in the available information.

Table 3.1.1 The list of the countries, time intervals and R^2 values for the linear correlation between daily diagnosis and the daily test numbers

Name of the country	The dates and related R^2 values
1. Argentine	Initial phase from 03/03/2020 to 18/05/2020 with $R^2 = 0.656$ Middle phase from 19/05/2020 to 08/08/2020 with $R^2 = 0.934$ Late phase from 09/08/2020 to 12/01/2021 with $R^2 = 0.487$
2. Bolivia	Initial phase from 15/03/2020 to 15/05/2020 with $R^2 = 0.769$ Middle phase from 16/05/2020 to 04/08/2020 with $R^2 = 0.901$ Late phase from 05/08/2020 to 14/01/2021 with $R^2 = 0.878$
3. Bulgaria	Initial phase from 02/05/2020 to 09/06/2020 with $R^2 = 0.0569$ Middle phase from 10/06/2020 to 17/08/2020 with $R^2 = 0.362$ Late phase from 18/08/2020 to 17/01/2021 with $R^2 = 0.190$
4. Chile	Initial phase from 10/04/2020 to 12/07/2020 with $R^2 = 0.531$ Middle phase from 13/07/2020 to 13/09/2020 with R2 = 0.000223 Late phase from 14/09/2020 to 17/01/2021 with $R^2 = 0.585$
5. Colombia	Initial phase from 06/06/2020 to 06/08/2020 with $R^2 = 0.845$ Middle phase from 07/08/2020 to 15/09/2020 with $R^2 = 0.613$ Late phase from 16/09/2020 to 17/01/2021 with $R^2 = 0.448$
6. Denmark	Initial phase from 08/03/2020 to 09/04/2020 with $R^2 = 0.742$ Middle phase from 10/04/2020 to 12/09/2020 with $R^2 = 0.161$ Late phase from 13/09/2020 to 14/01/2021 with $R^2 = 0.592$
7. France	Phase-Initial from 13/05/2020 to 17/07/2020 with $R^2 = 0.0344$ Middle phase from 18/07/2020 to 11/09/2020 with $R^2 = 0.358$ Phase-late from 12/09/2020 to 14/01/2021 with $R^2 = 0.0276$
8. Greece	Phase-Initial from 13/03/2020 to 28/07/2020 with $R^2 = 0.0974$ Middle phase from 29/07/2020 to 21/09/2020 with $R^2 = 0.0091$ Late phase from 22/09/2020 to 17/01/2021 with $R^2 = 0.58$
9. Guatemala	Phase-Initial from 19/03/2020 to 07/05/2020 with $R^2 = 0.295$ Middle phase from 08/05/2020 to 14/06/2020 with $R^2 = 0.165$ Phase-late from 15/06/2020 to 15/01/2021 with $R^2 = 0.0744$

10. Hungary	Phase-Initial from 13/03/2020 to 01/09/2020 with $R^2 = 0.0474$ Middle phase from 02/09/2020 to 13/10/2020 with $R^2 = 0.213$ Phase-late from 14/10/2020 to 17/01/2021 with $R^2 = 0.345$
11. Israel	Phase-Initial from 05/03/2020 to 01/06/2020 with $R^2 = 0.158$ Middle phase from 2020-06-02 to 15/11/2020 with $R^2 = 0.625$ Phase-late from 16/11/2020 to 11/01/2021 with $R^2 = 0.653$
12. Italy	Phase-Initial from 25/02/2020 to 25/03/2020 with $R^2 = 0.927$ Phase-Middle from 26/03/2020 to 06/10/2020 with $R^2 = 0.00121$ Phase-Late from 07/10/2020 to 17/01/2021 with $R^2 = 0.481$
13. Kazakhstan	Phase-Initial from 14/03/2020 to 17/05/2020 with $R^2 = 0.614$ Middle phase from 18/05/2020 to 01/07/2020 with $R^2 = 0.00470$ Phase-Late from 02/08/2020 to 13/01/2021 with $R^2 = 0.00215$
14. Mexico	Initial phase from 28/02/2020 to 22/04/2020 with $R^2 = 0.665$ Middle phase from23/04/2020 to 16/06/2020 with $R^2 = 0.527$ Late phase from 17/06/2020 to 16/01/2021 with $R^2 = 0.208$
15. Morocco	Initial phase from 16/03/2020 to 23/07/2020 with $R^2 = 0.194$ Middle phase from 24/07/2020 to 18/10/2020 with $R^2 = 0.734$ Late phase from 19/10/2020 to 15/01/2021 with $R^2 = 0.583$
16. Nepal	Phase-Initial from 11/03/2020 to 03/06/2020 with $R^2 = 0.556$ Middle phase from 04/06/2020 to 30/09/2020 with $R^2 = 0.608$ Late phase from 01/10/2020 to 15/01/2021 with $R^2 = 0.864$
17. Poland	Initial phase from 29/04/2020 to 22/05/2020 with $R^2 = 0.0420$ Middle phase from 23/05/2020 to 17/09/2020 with $R^2 = 0.218$ Late phase from 18/09/2020 to 16/01/2021 with $R^2 = 0.430$
18. Portugal	Initial phase from 4/3/2020 to 6/4/2020 with $R^2 = 0.798$ Middle phase from 7/4/2020 to 8/9/2020 with $R^2 = 0.00243$ Late phase from 9/9/2020 to 13/01/2021 with $R^2 = 0.435$
19. Romania	Initial phase from 13/03/2020 to 10/04/2020 with $R^2 = 0.609$ Middle phase from 11/04/2020 to 07/10/2020 with $R^2 = 0.640$ Later phase from 01/10/2020 to 10/01/2021 with $R^2 = 0.387$
20. Serbia	Initial phase from 10/03/2020 to 15/04/2020 with $R^2 = 0.831$

	Middle phase from 16/04/2020 to 25/10/2020 with $R^2 = 0.142$ Late phase from 26/10/2020 to 17/01/2021 with $R^2 = 0.876$
21. SouthAfrica	Initial phase from 12/03/2020 to 07/05/2020 with $R^2 = 0.902$ Middle phase from 08/05/2020 to 19/08/2020 with $R^2 = 0.825$ Later phase from 20/08/2020 to 17/0/2021 with $R^2 = 0.899$
22. UnitedKingdom	Phase-Initial from 31/03/2020 to 11/07/2020 with $R^2 = 0.678$ Middle phase from 12/07/2020 to 24/09/2020 with $R^2 = 0.714$ Late phase from 25/09/2020 to 14/01/2021 with $R^2 = 0.639$
23. US	Initial phase from 01/03/2020 to 31/03/2020 with $R^2 = 0.900$ Middle phase from 01/04/2020 to 20/10/2020 with $R^2 = 0.556$ Late phase from 21/10/2020 to 12/01/2021 with $R^2 = 0.225$

During the investigation of these time frames, these countries exhibited a distinct and evident weekly cycle in their data patterns. As an example, the linear correlation coefficients for the US are 0.900, 0.556, and 0.225 during the initial, middle, and late phases, respectively. The initial correlation coefficient aligns closely with the published data [49], but it notably decreases over time, almost disappears (see the Fig. 3.1.1). Upon examining the correlation coefficients of other countries, there's a notable variance observed (see the Fig. 3.1.2).

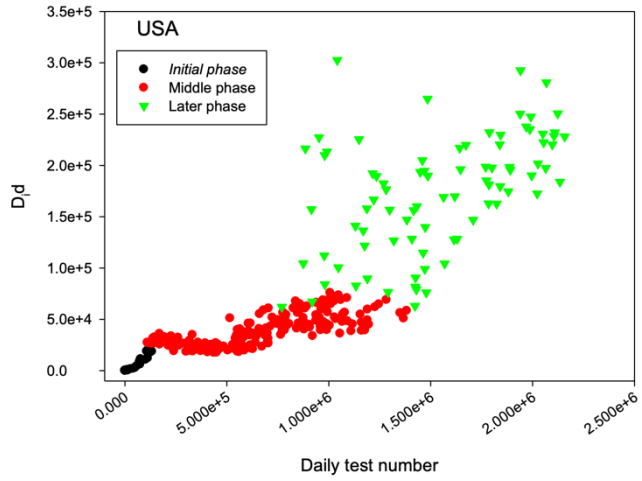

Figure 3.1.1 The time dependent linear correlation coefficients for different phases between the daily case and test number for US. As an example, for the determination of the time periods for the linear correlation coefficient determination, the data processing for the US is presented. The initial (01/03/2020 to 31/03/2020), middle (01/04/2020 to 20/10/2020) and late (21/10/2020 to 12/01/2021) phases are presented in black, red and green colors, respectively. The X- and Y- axes are daily test numbers and D_{id}, respectively.

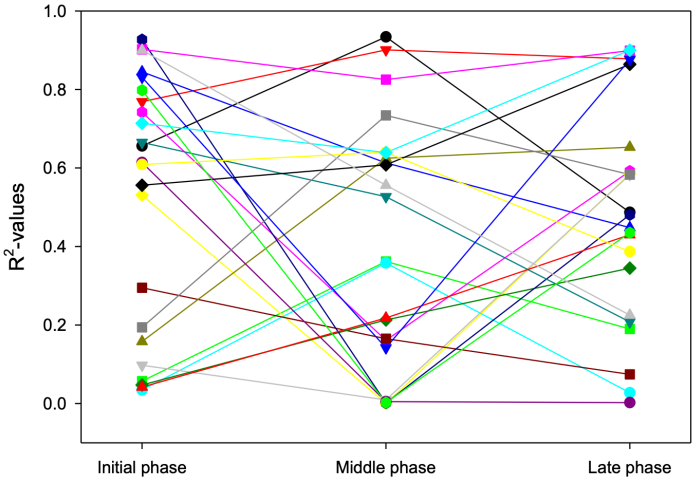

Figure 3.1.2 The time dependent linear correlation coefficients for different phases between the daily case and test number for 23 countries. The linear correlation between the daily case and test numbers for 23 countries at different time periods (Table 3.1.1) is presented in terms of R^2 values. These countries are Argentina Bolivia Bulgaria Chile Colombia Denmark France Greece Guatemala Hungary Israel Italy Kazakhstan Mexico Morocco Nepal Poland Portugal Romania Serbia South Africa United Kingdom and United States. Each color represents one country. The X- and Y- axes are phases and R_2 values, respectively.

Moreover, certain countries like Italy and the United States exhibit a more pronounced presence of WC in the later stages of the pandemic. This suggests that the high correlation observed in some countries at the beginning of the pandemic might be attributed to the stringent test protocols implemented by filiation teams working in the field and doctors due to early logistical challenges in test supply. Consequently, the observed linear correlation between WC and test numbers appears to be driven by D_{id} rather than the daily test number itself. Notably, a new recent studies acknowledge the presence of WC as a recognized phenomenon in D_{id} [49, 53] **but not on the daily infection numbers** and have already integrated it into pandemic simulations to develop new methodologies [54, 55].

3.2 The transmission of COVID-19 virus has WC with a minimum during the weekdays.

Most studies in the literature primarily concentrate on D_{id} rather than the time of virus infection. While these studies provide crucial insights into diagnosed cases, they overlook the specifics of virus transmission timing and the factors influencing it [56, 57]. In addition, these results can lead to misinforming the policy makers and public.

The virus transmission mechanism involves exposing a susceptible person to the virus, followed by an incubation period prior to the diagnosis of the infected individual. In the case of the SARS-CoV-2 virus, the minimum incubation period is around 3 days, and diagnosis peaks around the 6th day, extending up to 14 days post-infection. Various statistical models, such as contact tracing, location-based interaction studies between infectors and infectives, as well as diverse mathematical approaches, have contributed to these findings [50, 51]. Additionally, the day of diagnosis follows a Weibull distribution (Fig. 2.3.1) [52].

The Weibull distribution is frequently employed in analyzing daily new cases and deaths across countries with varying epidemic patterns. Known for its simplicity, effectiveness in modeling survival analysis data, and widespread availability in statistical software, it's a popular parametric lifetime model [58]. It is a posit that employing the Weibull distribution to model COVID-19 daily case and death data, along with other epidemic outbreaks, could yield crucial insights [58, 59]. These insights could serve as valuable support for governments and health authorities globally in implementing mitigation strategies.

Using these defined parameters, BTrac is developed to pinpoint the infection time. According to this, this I_{nt} is the result of daily D_{id} for 14 days with differential contributions. The findings reveal that I_{nt} exhibits a weekly cycle similar to D_{id} (Fig. 3.2.1). However, the time dependence of I_{nt}, exhibits a minimum during weekdays and maximum during the weekends in general (Fig. 3.2.1-3.2.3), contrasting with D_{id}, which peaks during weekdays. It is worth mentioning that D_{id} is utilized in almost all studies and policies were made based on this approach. At the relatively early times of the pandemic, the minimum for I_{nt} occurs on Tuesdays with the progression of pandemic and gradually shifts towards Fridays later on (Fig. 3.2.3). This shift can be attributed to the early NPIs and behavioral changes resulting from observations that virus transmission requires close human contact [60, 61]. Consequently, these weekly cycles are not controlled by the test numbers and therefore has to be controlled by some other factors such as NPIs and other human activity patterns.

The weekly cycle (WC) observed in I_{nt} holds significant insights into the daily dynamics of COVID-19 spread. To understand the information in detail and its time-dependent nature, I_{nt} for a given week is normalized against the I_{nt} on Monday of the same week (Fig. 3.2.3). For the statistical analysis, weekdays from Monday through Sunday are assigned numbers such as 1 through 7, respectively (Fig. 3.2.3). Analysis of

the normalized I_{nt} reveals a consistent weekly minimum, indicating a systematic temporal variation. For instance, Germany exhibits a pronounced WC (Fig. 3.2.1-3.2.2). Examining Germany's weekly minimums from March 16 to April 12, 2020—a relatively early phase of the SARS-CoV-2 pandemic—reveals a distinct trend (Fig. 3.2.2). The weekly minimum of I_{nt} initiates on Tuesdays and progressively shifts towards Fridays (Fig. 3.2.2). Overall, these findings illustrate that the normalized weekly minimum of I_{nt} divides the week into two halves, indicating the decreasing to increasing virus transmission phases (Fig. 3.2.3). This observed pattern could be influenced by weekly activities in work and social environments, encompassing homes and social gatherings. Furthermore, these observations indicate abrupt changes in virus spread, likely attributed to public awareness about the presence of virus and initial NPIs [62].

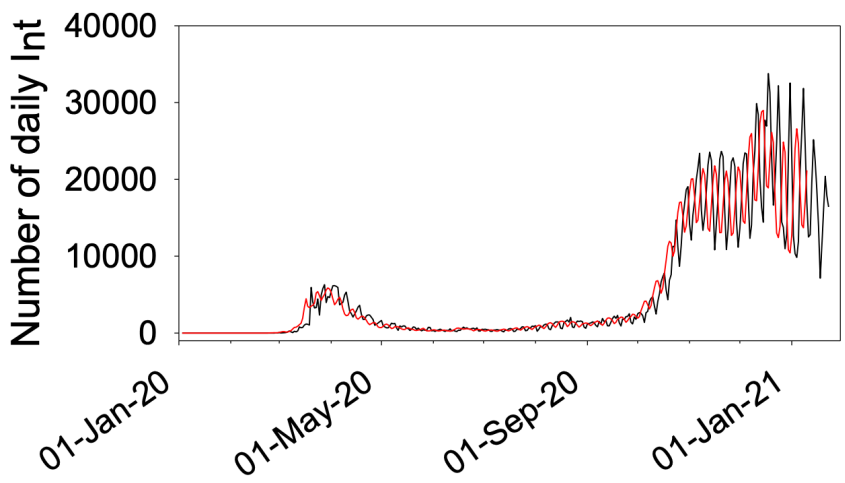

Figure 3.2.1 The conversion of the daily diagnosis number to daily infection number by BTrac and its time dependent variation. An example of transformed I_{nt} from D_{id} (black) to I_{nt} (red) for Germany is presented using BTrac. The X- and Y- axes represent the dates and number of daily infections, respectively.

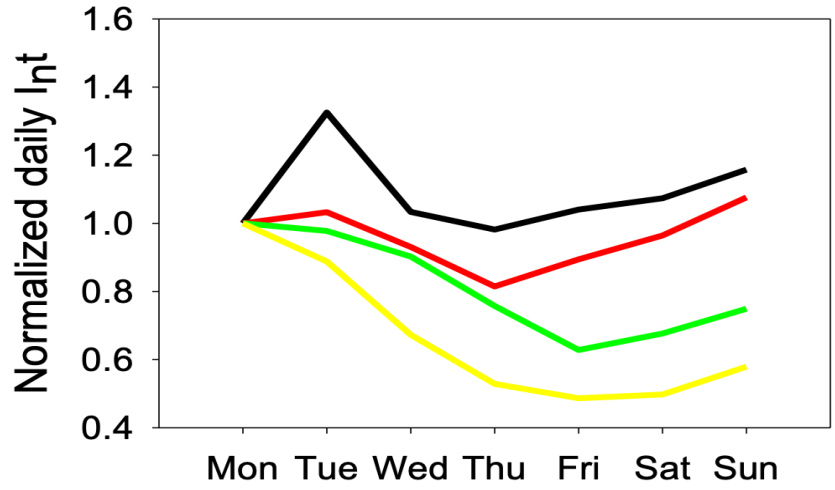

Figure 3.2.2 The conversion of the daily diagnosis number to daily transmission number by BTrac and its time dependent variation. I_{nt} is normalized by I_{nt} on Monday and normalized I_{nt} data for Germany is presented for the weeks starting at 16 March (black), 23 March (red), 30 March (green) and 6 April (yellow) 2020. The X- and Y- axes represent the days and value of normalized daily infection number, respectively.

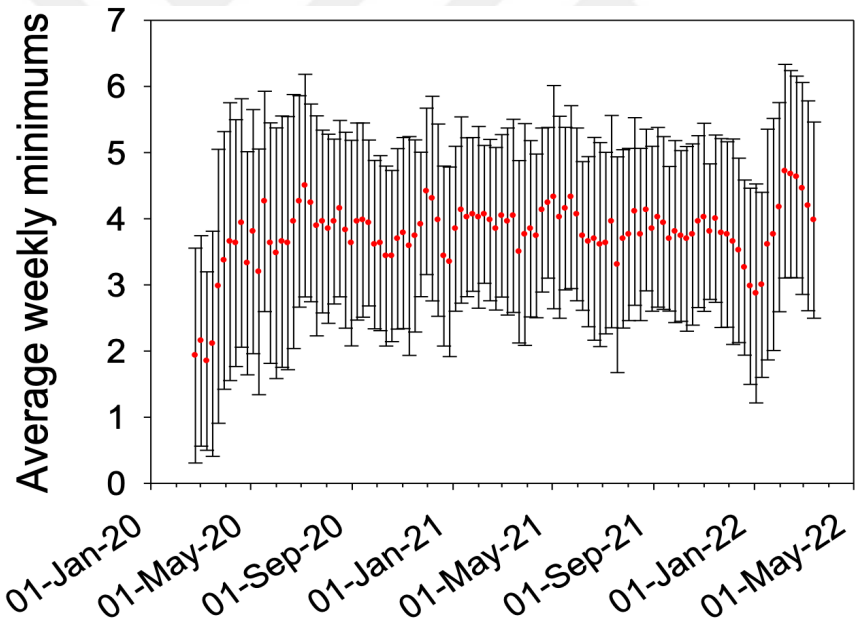

Figure 3.2.3 The conversion of the daily diagnosis number to daily transmission number by BTrac and its time dependent variation. The time dependence of the average weekly minimums (red) is presented for the 46 countries with the standard deviations. Numbers 1 to 7 refer to Monday to Sunday respectively. The X- and Y- axes represent dates and the day corresponding to the average weekly minimum, respectively.

3.3 The R_0 values of infection also has WC driven human activities

The investigation for 46 countries into the presence of a WC was extended to examine R_{0i}, revealing a clear time-dependent pattern resembling I_{nt} but with less variability (Fig. 3.3.1). R_{0i} consistently peaks on Saturdays for 40 out of 52 weeks and hits minimum on Wednesdays for 45 out of 52 weeks. Notably, the weekly minimum shifts to Tuesdays during the Christmas and New Year week of 2020, with R_{0i} starting to increase a day before the holiday period begins. These findings effectively capture the impact of human activities prompted by holidays and underscore the efficacy of this new methodology in grasping the dynamics of COVID-19 virus spread.

In general, R_{0i} tends to rise after Wednesdays, aligning well with the three-day virus incubation period starting from Mondays—the onset of the workweek—reaching its peak on Saturdays. This indicates the synergistic transmission between work and social environments, forming a loop broken on Sundays, causing a decline in R_{0i} until Thursdays. Moreover, the maximum R_{0i} values per week increase while the minimum R_{0i} values decrease, indicating a widening gap between them as the pandemic progresses. Considering that the continuous evolution and propagation processes of viruses are based on their interactions with their hosts and environmental factors, this result indicates the increasing infection potential of the virus under the increasing pressure of NPIs.

In conclusion, the COVID-19 virus displays variable R_{0i} values exhibiting a WC driven by the interplay between transmission in social and work environments. With the progression of pandemic, the virus evolves in terms of its infective capacity, influenced by the changing dynamics of social interaction and intervention strategies.

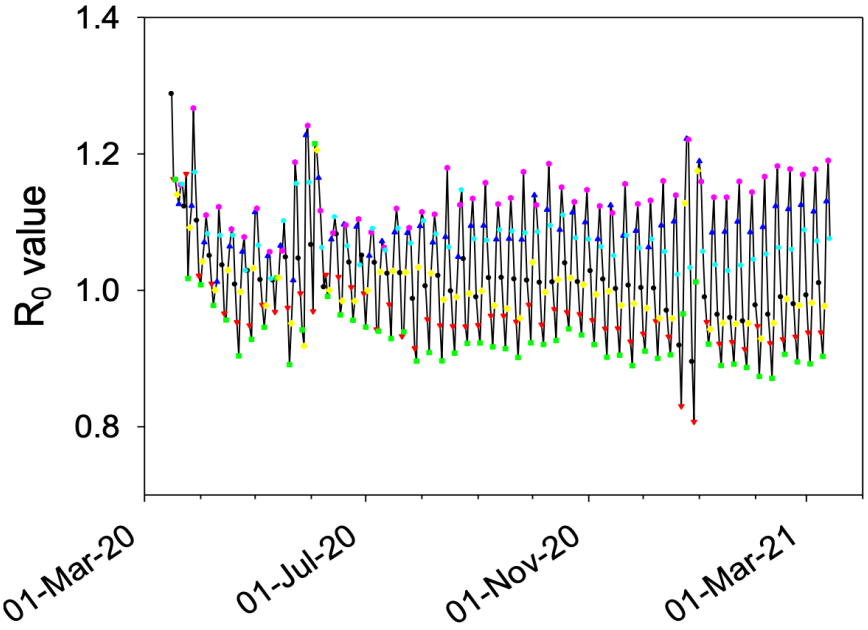

Figure 3.3.1 The variation of R_{0i} values with respect to the progression of pandemic. The time dependence of R_0s (black line) at different days for 46 countries are presented from Monday to Saturday with the color of black, red, green, blue, pink and cyan, respectively. The X- and Y- axes represent the dates and R_{0i} values, respectively.

3.4 The effect of the national holidays on WC as a social factor

Continuing the exploration of potential impact of human behaviors on the weekly minimum of I_{nt} and to validate the developed BTrack model, major holidays like Christmas, New Year, and the Festival of Sacrifice were chosen. These holidays are observed by different countries, with Christmas and the Festival of Sacrifice observed in various nations, while New Year is a global celebration. The selection also considers the Christmas celebration on Thursday, December 24, 2020, followed by New Year's celebration on Thursday, December 31, 2020. Moreover, the Festival of Sacrifice, observed on Tuesday, June 20, 2021. It is worth to mention that the Festival of Sacrifice is relatively isolated from other national holidays. These choices provide an opportunity to demonstrate the BTrack model's capability, yet it poses a challenge in isolating their individual effects of the Christmas and new year celebrations on the weekly minimum of I_{nt} due to their proximity to each other, data irregularities, and the diverse religious observances across countries.

To distinguish between the effects of Christmas and New Year holidays, the data is categorized based on the predominant religion belief in each country. Countries where more than 50% of the population follows the Christian faith are classified as Christian countries, and thus expected to observe the Christmas holiday (See table 3.4.1).

Table 3.4.1 Religious faith of the countries

Christian countries	Non- Christian countries	Muslim countries	Non- Muslim countries
Argentina	Azerbaijan	Azerbaijan	Argentina
Armenia	Bangladesh	Bangladesh	Armenia
Austria	Egypt	Egypt	Austria
Belarus	India	Indonesia	Belarus
Brazil	Indonesia	Iran	Brazil
Bulgaria	Iran	Iraq	Bulgaria
Canada	Irak	Kazakhstan	Canada
Chile	Israel	Lebanon	Chile
Colombia	Kazakhstan	Morocco	Colombia
Croatia	Lebanon	Nigeria	Croatia
Czechia	Morocco	Pakistan	Czechia
Dominican Republic	Nigeria	Saudi Arabia	Dominican Republic
France	Pakistan	Turkey	France
Germany	Saudi Arabia	United Arab Emirates	Germany
Greece	Turkey		Greece
Guatemala	UAE		Guatemala
Hungary			Hungary
Italy			India
Japan			Israel
Mexico			Italy
Norway			Japan
Poland			Mexico
Potugal			Norway
Romania			Poland
Russia			Portugal
Serbia			Romania

South Africa			Russia
Spain			Serbia
UK			South Africa
US			Spain
			United Kingdom
			United States

To examine the impact of the Christmas and New Year holidays, the weekly minimums of I_{nt} were analyzed for 46 countries (Table 3.4.1 for the list of countries) across six weeks, from December 7, 2020, to January 8, 2021, to demonstrate the change in weekly minimum trends. A distinct trend emerged in the weekly minimums during this period (Fig. 3.4.1). Specifically, it remained consistent on Thursdays during the weeks starting December 7 and 14, 2020 (mean ± SD 4.326 ± 0.2368 vs 4.022 ± 0.2002; P = 0.2375), and then shifted to Wednesdays for the weeks starting December 14 to 21, 2020. This shift perfectly coincides with human behavior related to holiday celebrations commencing on Wednesdays. This change was statistically significant (4.02 ± 1.36 vs 3.41 ± 1.28; P = 0.0033) (see Table 3.4.2). The trend persisted, moving toward the middle of the week, but the difference between the weeks starting on December 21 and 28, 2020, was not significant (4.022 ± 0.2002 vs 3.130 ± 0.1775; P = 0.1201). Toward the end of the holiday season, the weekly minimum reverted from Wednesday back to Thursday for the weeks starting on December 28, 2020, to January 4, 2021, and this change was statistically significant (3.130 ± 0.1775 vs 3.891 ± 0.1971; P = 0.0005). For the subsequent weeks starting on January 4 and 11, 2021, the trend continued, but it was not statistically significant (3.891 ± 0.1971 vs 4.174 ± 0.2092; P = 0.1360).

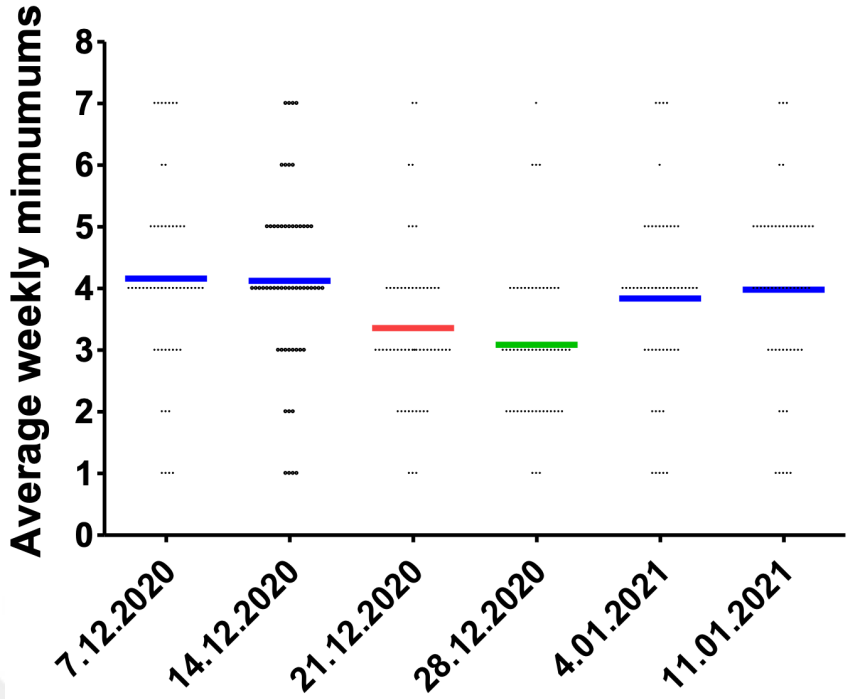

Figure 3.4.1 The effect of the Christmas and New Year holidays on the worldwide weekly minimums of I_{nf}. The time dependent change of the weekly minimum in average for 46 countries, is presented where the blue colored lines are the averages for the weeks before the Christmas (red) and after the New Year (green). Numbers 1 to 7 refer to Monday to Sunday respectively. The X- and Y- axes represent the dates and the day corresponding to the average weekly minimum, respectively.

Table 3.4.2 The effect of the Christmas and New Year holiday on the minimum of the weekly cycle using Student's t-test

	The beginning day of the week	7.12.2020	14.12.2020	21.12.2020	28.12.2020	4.01.2021	11.01.2021
All countries (n=46)	Mean ± SD	4.33 ± 1.61	4.02 ± 1.36	3.41 ± 1.28	3.13 ± 1.20	3.89 ± 1.34	4.17 ± 1.42
	P-value	0.2375		0.1201		0.1360	
			0.0033		0.0005		
Christian countries(n=30)	Mean ± SD	4.47 ± 1.46	4.10 ± 1.10	3.20 ± 1.06	3.03 ± 1.27	3.97 ± 1.10	4.30 ± 1.12
	P-value	0.2013		0.2027		0.2712	
			0.0030		0.0060		
Non-Christian countries (n=16)	Mean ± SD	4.06 ± 1.88	3.88 ± 1.7842	3.81 ± 1.56	3.31 ± 1.08	3.75 ± 1.73	3.94 ± 1.88
	P-value	0.4472		0.2074		0.3667	
			0.3318		0.1711		

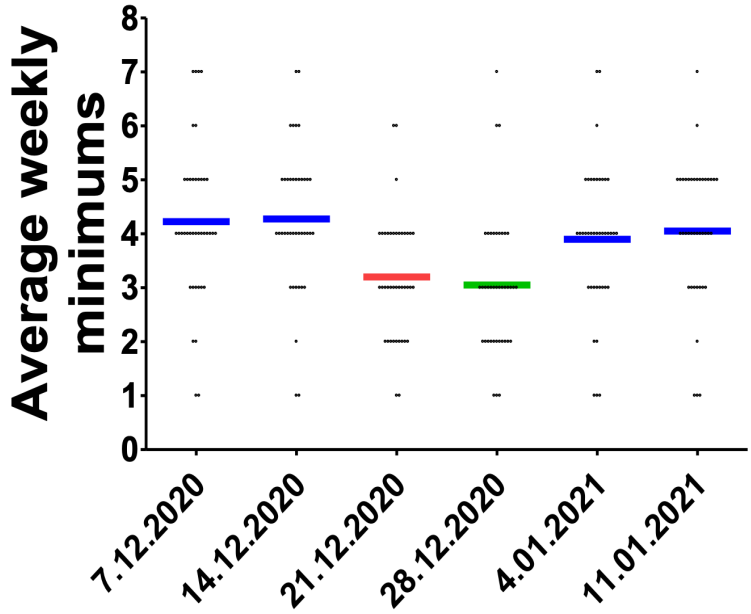

Figure 3.4.2 The effect of the Christmas and New Year on the weekly minimums of I_{nf} for Cristian countries. The same values as in Fig 3.4.1 are presented for the Christian countries.

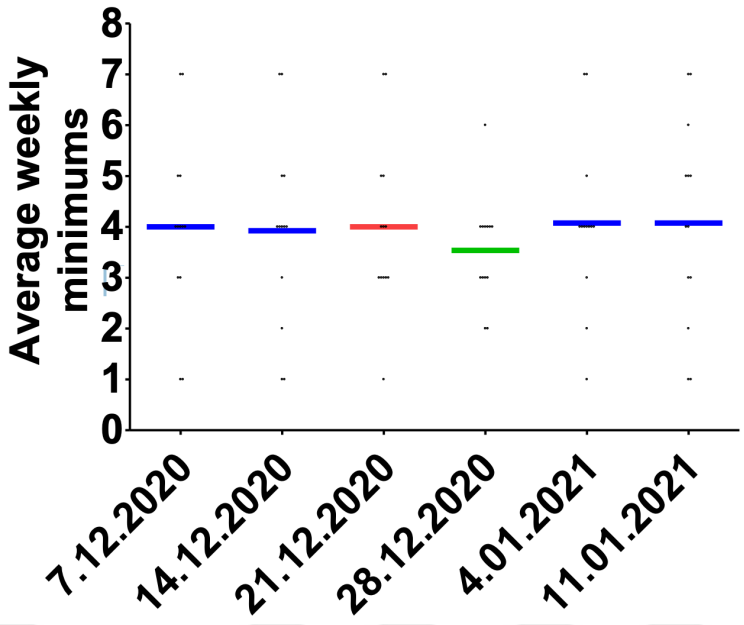

Figure 3.4.3 The effect of the Christmas and New Year on the weekly minimums of I_{nt} for non-Cristian countries. The same values as in Fig 3.4.1 presented for non-Christian countries.

The observed trends and statistical variances, as previously outlined, become more pronounced within the group of Christian countries (n = 30) (for December 21 and 28, 2020 (3.20 ± 1.06 vs 3.03 ± 1.27; P = 0.2027)) (Fig. 3.4.2, see table 3.4.2). Conversely, the trend among non-Christian countries (n = 16) dissipates, (for December 21 and 28, 2020 (3.81 ± 1.56 vs 3.31 ± 1.08; P = 0.2074)) while the trend linked to New Year persists (Fig. 3.4.3, see Table 3.4.2).

These findings underscore the efficacy of the developed BTrack methodology in revealing the adverse impact of these two holidays on COVID-19 virus transmission.

Furthermore, the impact of holidays was further explored, specifically focusing on the Feast of Sacrifice between July 5 and August 8, 2021, over five weeks, including the third week with the Feast of Sacrifice holiday. Among the 46 countries analyzed, the weekly minimum during the week of the holiday displays statistical differences compared to the preceding week (3.6536 ± 2.8873 vs 3.9565 ± 1.6049; P = 0.0467), while the remaining weeks don't exhibit such distinctions (Fig. 3.4.4, Table 3.4.3).

When countries are categorized based on religious affiliation, those where 50% or more of the population follows the Muslim faith are classified as Muslim countries, while the remaining are grouped as non-Muslim countries. Among the Muslim countries (n = 14), the weekly minimum shifts from Thursday to Wednesday before and then back to Thursday after the Feast of Sacrifice celebration, which commenced on July 20, 2021.

These transitions were found to be statistically significant (4.2143 ± 2.2250 vs 2.3571 ± 1.9457; P = 0.0134 and 2.3571 ± 1.9457 vs 3.4286 ± 1.5046; P = 0.0310, respectively) (Fig. 3.4.5, Table 3.4.3). Conversely, for the non-Muslim countries (n = 32), there are no statistically significant changes observed (Fig. 3.4.6, see Table 3.4.3). Notably, during the week of the holiday, the weekly minimum falls on Tuesday, coinciding with the official start of the Feast of Sacrifice celebration.

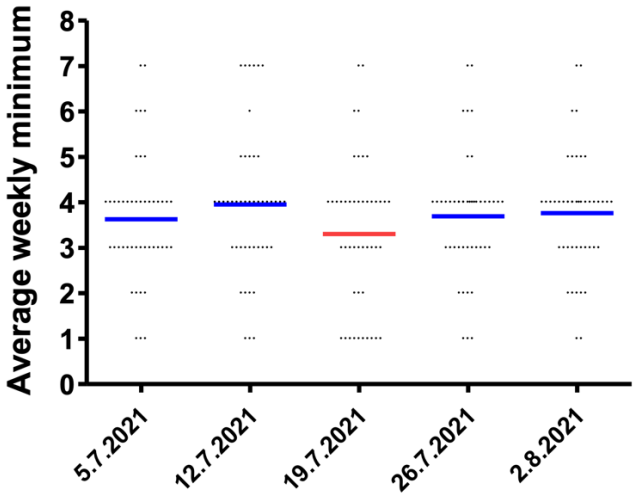

Figure 3.4.4 The effect of the Feast of the Sacrifice holidays on the minimum of the weekly cycle on I_{nt}. The time dependent change of the weekly minimum in average for 46 countries is presented where the blue colored lines are the averages for the weeks before and after the Feast of Sacrifice (red). Numbers 1 to 7 refer to Monday to Sunday respectively. The X- and Y- axes represent the dates and the day corresponding to the average weekly minimum, respectively.

Table 3.4.3 The effect of the Feast of sacrifice holiday on the minimum of the weekly cycle using Student's t-test

	The beginning day of the week	05.07.2021	12.07.2021	19.07.2021	26.07.2021	02.08.2021
All the countries (n=46)	Mean ± SD	3.6304±1.3721	3.9565±1.6049	3.3043 ± 1.6312	3.6957 ±1.3477	3.760 ±1.3027
	P-value	0.1520		0.1358		
			0.0467		0.3781	
Muslim countries (n=14)	Mean ± SD	3.0714±1.6392	4.2143±2.2250	2.3571±1.9457	3.4286±1.5046	3.5714±1.7852
	P-value	0.0870		0.0310		
			0.0134		0.4724	
Non-Muslim countries (n=32)	Mean ± SD	3.8750 ±1.1846	3.8438 ±1.2728	3.7188 ± 1.3010	3.8125 ±1.2811	3.8438 ±1.0506
	P-value	0.4973		0.3855		
			0.3960		0.3880	

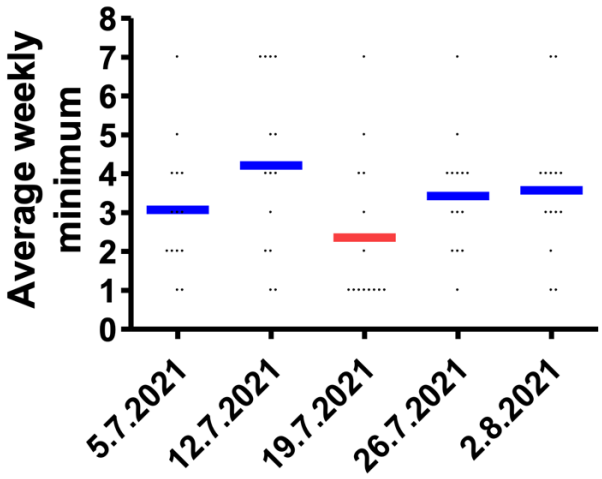

Figure 3.4.5 The effect of the Feast of the Sacrifice holidays on the minimum of the weekly cycle on I_{nt} for the Muslim countries. The same value as in Fig 3.4.4 is presented for the Muslim countries.

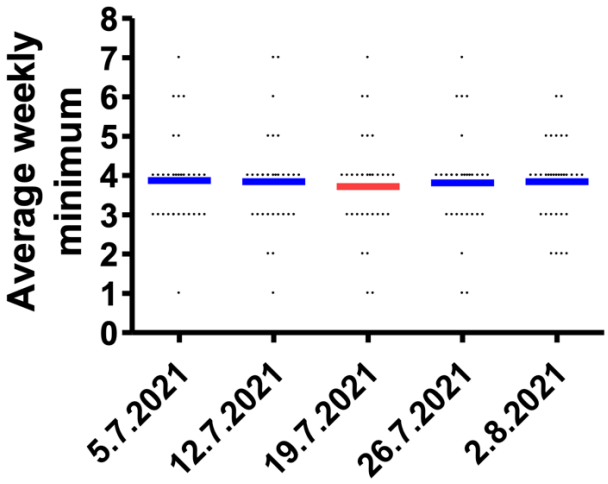

Figure 3.4.6 The effect of the Feast of the Sacrifice holidays on the minimum of the weekly cycle on I_{nt} for the non-Muslim countries. The same value as in Fig 3.4.4 is presented for the non-Muslim countries.

These findings confirm that the transmission of COVID-19 virus increases during holidays, similar to the observations from Christmas, New Year, and Feast of Sacrifice celebrations. They also demonstrate the efficacy of the new model in tracing back the impact of holidays from daily case numbers and identifying the relaxed human behavior during holidays as a contributing factor to the virus spread among family and friends. So, these results start shedding the light on what controls the weekly cycle on the daily infection number as well as D_{id}, therefore on the daily infection numbers as an important factor which aligns well with the observation using daily case numbers.

3.5 The trends on the weekly minimum of I_{nt} during the increasing and decreasing phases of the pandemic.

To thorough exploration on the fluctuations of the weekly minimum on I_{nt} during the ascending and descending phases of three peaks in the SARS-CoV-2 pandemic, data from 46 countries is re-examined. These countries exhibit peaks in D_{id} on varying dates due to each country's unique characteristics. The dates of these peaks are chosen according to the rising and falling phases (refer to Table 2.3.1 for the list of countries and related dates). Subsequently, after transforming D_{id} into I_{nt} and normalizing it as previously described, the data is divided into six blocks, each comprising four weeks. Three of these blocks correspond to the rising phases, while the remaining three pertain to the declining phases of the consecutive three peaks in virus spread, aimed at clearly capturing discernible trends (Fig. 3.5.1).

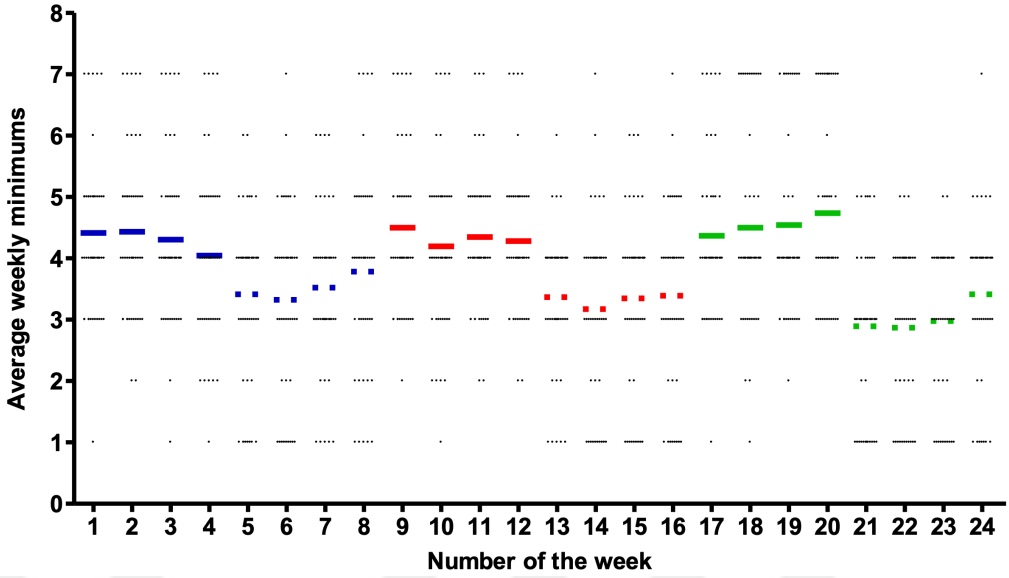

Figure 3.5.1 The variation on the weekly minimum during the increasing and decreasing phase of the peaks. The variation on the weekly minimums is presented as an average for the initial (blue), middle (red) and late (green) phases where the solid lines and doted lines belong to decreasing and increasing phases of three different peaks of COVID-19 pandemics, respectively. Numbers 1 to 7 refer to Monday to Sunday respectively. The X- and Y- axes represent the week numbers and the day corresponding to the average weekly minimum, respectively.

The outcomes indicate that the minimum values per week fluctuate between Wednesday and Thursday during growth and between Thursday and Friday during decline phases (Fig. 3.5.1). The difference between these phases is notably significant (3.2899 ± 0.2687 versus 4.3895 ± 0.1787, with $P < 0.0001$, respectively). There's a significant pattern during the growth phases (Spearman's $\rho = -0.09570$, $P = 0.0123$), showing a shift of the weekly minimum towards Wednesday. However, this shift isn't statistically significant during the declining phases (Spearman's $\rho = 0.03141$, $P = 0.2307$), indicating a weekly minimum shift towards Friday.

Based on the earlier results from holidays and daily infection numbers, these results emphasize the significant impact of human interactions in work and social environments, with a reduced and/or strict human interaction during decreasing phases and more relaxed interactions during increasing phases. Consequently, the shifts in human behavior and activities play a crucial role in determining the progression of pandemics. Furthermore, these findings suggest that the difference between these two trends becomes more distinct as the time advances, indicating that both individuals and

governments learned to protect the public more effectively from COVID-19 infection as the time progressed.

Notably, during the decreasing phases, the shift of the weekly minimum towards Friday likely stems from the successful implementation of NPIs, particularly restrictions in workplaces aimed at curbing virus transmission. It's intriguing to note that a mere one-day change in the weekly minimum can signify shift from increasing to decreasing phases in the pandemic progression, highlighting the significance of the day with the weekly minimum as a reliable indicator for the progression of pandemics.

3.6 The effect of the socio-economic factors on the weekly cycle and therefore the COVID-19 pandemic

Understanding the socio-economic factors influencing COVID-19 transmission is crucial for managing the current pandemic and potential future pandemics. Expanding on the efficacy of this new model in capturing holiday effects on virus spread, suspected socio-economic factors such as GDP, GDP per capita, GINI index for income inequality, and HDI are analyzed concerning COVID-19 spread at early (2nd to 29th March 2020), middle (1st to 28th March 2021), and later (21st February to 20th March 2022) times.

Datasets for GDP, GDP per capita, GINI index, and HDI were obtained from the World Bank, World Population Review and United Nations Development Programme websites. Assigning numerical values to the days of the week, the weekly minimums for each country in four-week blocks across different pandemic periods were determined and added to capture the general trends. Subsequently, correlations between these aggregate weekly minimum scores and socio-economic factors were investigated.

Among these factors, GDP per capita and HDI displayed negative correlations with the aggregated values during early ($r_s = -0.2814$, $p = 0.0291$ and $r_s = -0.2787$, $p = 0.0304$, respectively) and later times ($r_s = -0.5041$, $p = 0.0002$ and $r_s = -0.4969$, $p = 0.0002$, respectively) (see Table 3.6.1). This suggests that as GDP per capita and HDI increase, the weekly minimums move toward the latter half of the weekdays, indicating a decrease in COVID-19 spread. In essence, these findings underscore the adverse impact of known disparities linked to individual income and education on virus transmission.

Table 3.6.1 Socio-economic factors Correlation of the possible factors with weekly minimums for 46 countries

	GDP	GDP per capita	GNI index	HDI
Total scores for the weeks	Spearman r 95% confidence interval P value	Spearman r 95% confidence interval P value	Spearman r 95% confidence interval P value	Spearman r 95% confidence interval P value
2-23 March 2020	-0.242 -0.504 to 0.0611 0.0528	-0.281 -0.535 to 0.0186 0.0291	-0.117 -0.405 to 0.191 0.221	-0.279 -0.533 to 0.0215 0.0304
1-22 March 2021	-0.0624 -0.354 to 0.241 0.340	0.107 -0.198 to 0.393 0.240	-0.407 -0.778 to 0.175 0.0743	0.0551 -0.247 to 0.348 0.358
21 February – 14 March 2022	0.0391 -0.262 to 0.334 0.398	-0.504 -0.698 to -0.242 0.0002	-0.0423 -0.340 to 0.263 0.3913	-0.497 -0.693 to -0.233 0.0002

Further exploring these correlations, countries were stratified based on GDP levels: higher GDP (n = 20) and lower GDP (n = 26) categories and evaluated using spearman rho correlation. There are clear variations in the correlations noticed among these two sets of countries.

The countries (n = 20) with the higher GDP in 2020 are Argentina, Austria, Brazil, Canada, France, Germany, India, Indonesia, Israel, Italy, Japan, Mexico, Nigeria, Poland, Russia, Saudi Arabia, Spain, Turkey, United Kingdom and United States. The countries (n = 26) with the lower GDP in 2020 are Armenia, Azerbaijan, Bangladesh, Belarus, Bulgaria, Chile, Colombia, Croatia, Czechia, Dominican Republic, Egypt, Greece, Guatemala, Hungary, Iran, Iraq, Kazakhstan, Lebanon, Morocco, Norway, Pakistan, Portugal, Romania, Serbia, South Africa and United Arab Emirates.

There's a notable disparity in correlations between these country groups. For the top 20 countries with higher GDP, correlations between GDPs per capita, HDI, and the aggregate weekly minimum values are solely evident in the final time block (rs = -0.6335, p = 0.0014 and rs = -0.6358, p = 0.0013, respectively) (refer to Table 3.6.2). In contrast, for the 26 countries with lower GDP, these correlations are present in both early (rs = -

0.3803, p = 0.0277 and rs = -0.3334, p = 0.0480, respectively) and final time periods (rs = -0.4386, p = 0.0125 and rs = -0.4296, p = 0.0143, respectively).

Table 3.6.2 Socio-economic factors Correlation of the possible factors with weekly minimums for top 20 countries withhighest GDP at 2020

Total scores for the weeks	**GDP** Spearman r 95% confidence interval P value	**GDP per capita** Spearman r 95% confidence interval P value	**GNI index** Spearman r 95% confidence interval P value	**HDI** Spearman r 95% confidence interval P value
2-23 March 2020	0.0137 -0.442 to 0.465 0.477	-0.0761 -0.512 to 0.391 0.375	-0.0822 -0.528 to 0.399 0.369	-0.140 -0.559 to 0.335 0.278
1-22 March 2021	-0.0722 -0.509 to 0.395 0.381	0.0327 -0.428 to 0.479 0.446	-0.107 -0.546 to 0.377 0.331	-0.0600 -0.500 to 0.405 0.401
21 February – 14 March 2022	0.00923 -0.447 to 0.461 0.4846	-0.634 -0.845 to -0.252 0.00140	0.140 -0.349 to 0.568 0.284	-0.636 -0.846 to -0.256 0.00130

Table 3.6.3 Correlation of the possible factors with weekly minimums for 26 countries with lower GDP at 2020

Total scores for the weeks	**GDP** Spearman r 95% confidence interval P value	**GDP per capita** Spearman r 95% confidence interval P value	**GNI index** Spearman r 95% confidence interval P value	**HDI** Spearman r 95% confidence interval P value
2-23 March 2020	-0.0826 -0.465 to 0.326 0.344	-0.380 -0.676 to 0.0205 0.0277	-0.00482 -0.402 to 0.394 0.491	-0.333 -0.646 to 0.0741 0.0480
1-22 March 2021	-0.148 -0.515 to 0.265 0.235	0.316 -0.0935 to 0.634 0.0580	0.00657 -0.392 to 0.403 0.487	0.227 -0.188 to 0.573 0.133
21 February – 14 March 2022	0.311 -0.0993 to 0.630 0.0613	-0.439 -0.712 to -0.0495 0.0125	-0.0751 -0.459 to 0.333 0.358	-0.430 -0.707 to -0.0385 0.0143

These findings highlight that GDP per capita hold more significant in determining virus spread than overall GDP. This is further supported by the presence and absence of correlation between GDP per capitas and weekly minimum of I_{nt} for lower GDP and higher GDP country groups, respectively. As a conclusion, individual economic activity on the weekly basis seems to negatively impact the pandemic. It's essential to reiterate that virus spread appears to be independent of GDP but linked to GDP per capita, according to the presented results.

3.7 Simulation with the variable R_{0i} values replicate the weekly cycles on the real-world data.

The data presented here strongly indicates that the WC significantly influences the spread of the COVID-19 virus due to the fluctuations in daily socio-economic human activities throughout the week. This prompts the hypothesis that variations in the R_{0i} value is the underlying cause of the WC observed in I_{nt} and consequently, D_{id}. While viral mutations might contribute to daily variations in WC, they follow a regular pattern that is unlikely to be solely explained by virus mutations within such a short timeframe.

Drawing from these findings, a Variable R_{0i} ($VarR_{0i}$) Model is devised to capture the impact of human activities on COVID-19 transmission. This model aims to evaluate how this cycle influences the virus spread by employing a reverse application of the BTrack model, utilizing forward tracing methodologies (Fig. 3.7.1 – 3.7.2).

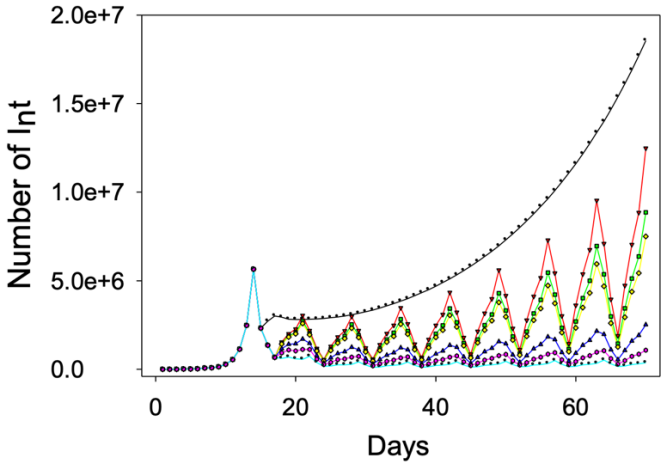

Figure 3.7.1 Simulation for the daily infection of the COVID-19 virus using $VarR_{0i}$ model. The forward tracking of I_{nt} using the $VarR_0$ model with constant R_{0i} (black) and variable R_{0i} which is presented with the progressive decrease with 0 (red), 5 (green), 7.5 (yellow), 25 (blue), 40 (pink) and 60% (cyan) on Thursday through Sunday. The X- and Y axes represent the number of the day and number of the daily infection, respectively.

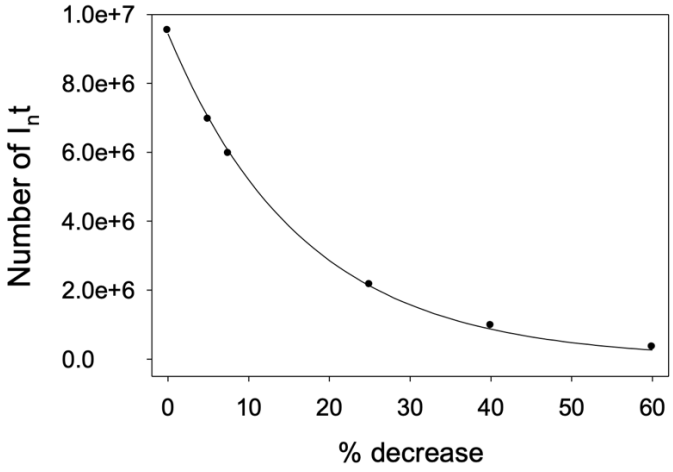

Figure 3.7.2 Simulation for the daily transmission of the SARS-CoV-2 using VarR0 model. The relation between % decrease and I_{nt} is presented. The X- and Y- axes represent the percentage decrease and the daily number of infections, respectively.

Following the initial two weeks, the simulation maintains constant R_{0i} values or gradually decreases them from 0 to 60% on Thu, Fri, Sat, and Sun for an additional 8 weeks. However, R_{0i} values remain constant on Mon, Tue, and Wed. This decision is informed by data

from the pandemic's increasing and decreasing phases, aligning with patterns observed up to Thu (Fig. 3.5.1).

Results indicate that simulations incorporating variable R_{0i} values successfully replicate the observed WC of D_{id}, mirroring real-life data. Conversely, simulations using a constant R_0 value fail to replicate this weekly cycle (Fig. 3.7.3).

The simulations initially begin with 1000 infected individuals and a considerably large population without prior exposure to the virus. Comparing simulations using a constant R_{0i} value of 0.24 with those employing variable R_{0i} values (0.24 and alternating values of 0.12, 0.06, 0.18, 0.30, 0.36, and 0.42 from Mon to Sun) for the following seven weeks, notable differences emerge. The variable R_{0i} simulation predicts 9.52 million I_{nt}, 29.6 million I_t, and 2.65 million D_{id}, while the constant R_{0i} simulation forecasts 13.4 million I_{nt}, 58.6 million I_t, and 10.7 million D_{id}, despite both simulations averaging an R_{0i} value of 0.24.

This discrepancy suggests that simulations utilizing a constant R_{0i} value tend to overestimate I_{nt}, I_t, and D_{id} or underestimate the actual R_{0i} value. This disparity could stem from differing definitions; while R_{0i} is occasionally defined as the total secondary infections caused by one infected individual, in many studies, D_{id} is commonly used rather than the total infected but undiagnosed individuals capable of virus transmission. Hence, this data underscores the importance of employing a variable R_{0i} value approach instead of a constant R_{0i} value for a more accurate evaluation of the pandemic and for improved estimations.

Further analysis involves systematically reducing the variable R_{0i} values by 5, 7.5, 25, 40, and 60% on Thu, Fri, Sat, and Sun over an additional 8 weeks, while maintaining a constant baseline variable R_{0i} value from Mon to Sun, respectively (Fig. 3.7.1 and materials Fig. 3.7.3-3.7.4). At the seven-week mark following the initial two weeks, applying a first-order exponential decay equation suggests that I_{nt}, I_t, and D_{id} halve when reductions of 11.6%, 13.9%, and 13.9% are imposed on the latter half of the week starting on Thursday.

Consequently, the VarR_{0i} model accurately mirrors the progression of the SARS-CoV-2 virus pandemic concerning WC and provides improved predictions for pandemic progression. Thus, the VarR_{0i} model stands as a more reliable tool for real-life preparation efforts.

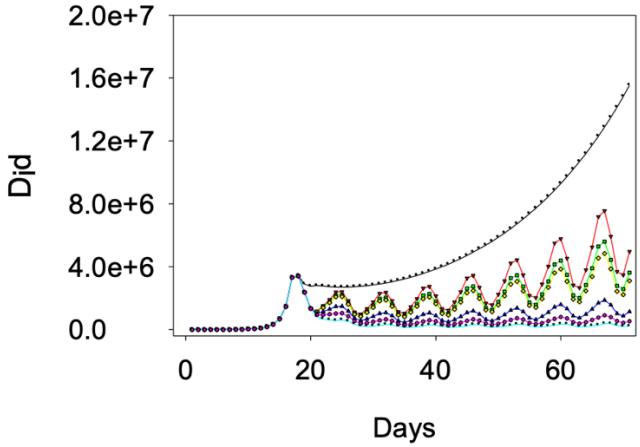

Figure 3.7.3 Simulation using $VarR_{0i}$ model for the daily total infected and diagnosed people. The forward tracking of $Di\ d$ using the $VarR_{0i}$ model with constant R_{0i} (black) and variable R_{0i} which is presented with the progressive decrease with 0 (red), 5 (green), 7.5 (yellow), 25 (blue), 40 (pink) and 60% (cyan) on Thursday through Sunday. The X- and Y axes represent the number of the day and number of the daily infection, respectively.

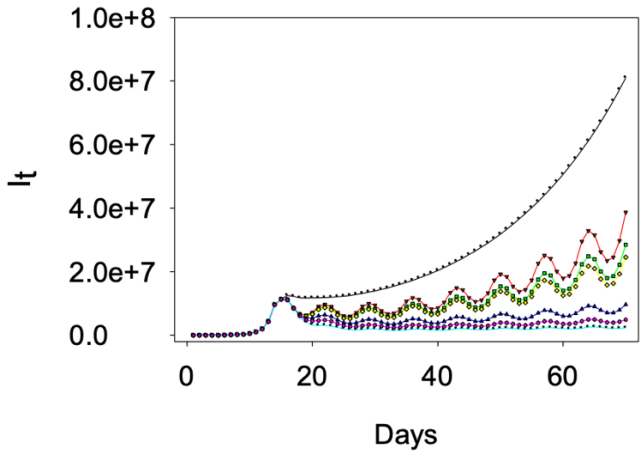

Figure 3.7.4 Simulation using $VarR_{0i}$ model for the daily total infected and diagnosed people. The relation between % decrease and f D_{id} is presented.

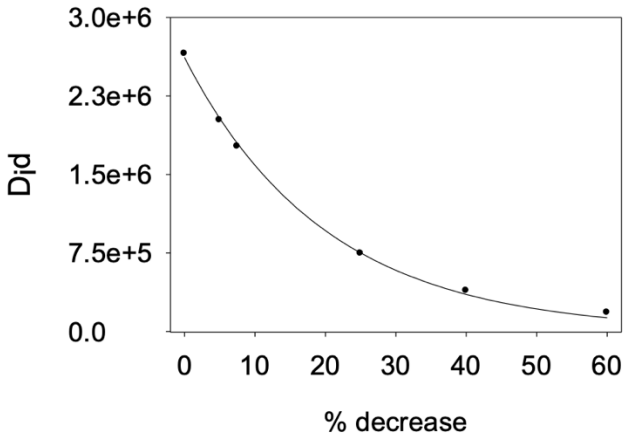

Figure 3.7.5 Simulation using $VarR_{0i}$ model for the daily total infected and diagnosed people. The same values as in Fig 3.7.3 for total infected but not diagnosed population (I_t).

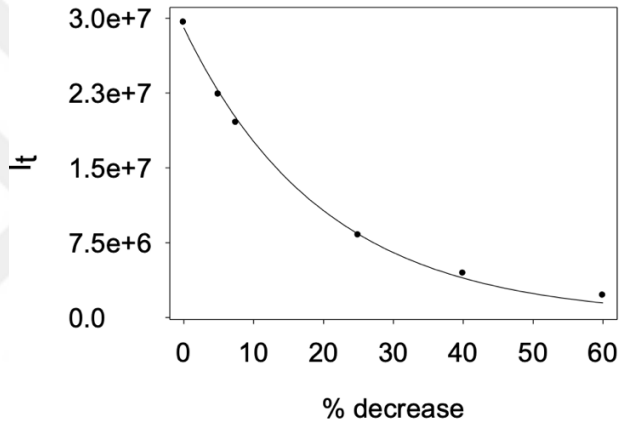

Figure 3.7.6 Simulation using $VarR_{0i}$ model for the daily total infected and diagnosed people. The same values as in Fig 3.7.4 for total infected but not diagnosed population (I_t).

Chapter 4

CONCLUSIONS AND FUTURE PROSPECTS

4.1 Conclusions

Almost all prior models have primarily focused on D_{id}, contributing significantly to our comprehension and simulation of pandemic progression to inform the policy makers and public. However, they often overlook the critical factor of transmission timing, which profoundly influences virus propagation and the formulation of effective control strategies. This study introduces a novel method called BTrack, which successfully determines infection timing from D_{id} data. So it is expected that this new model will provide more relevant data to inform policy makers and better control for the future pandemics.

Through BTrack, the time-dependent characteristics of I_{nt} and R_{0i} are identified, displaying a weekly cyclic pattern mirroring that of D_{id}. Notably, the weekly minimum of R_{0i} remains relatively constant on Wednesdays, aligning perfectly with the three-day incubation period, signifying that individuals become effective infectors after three days.

In contrast, the weekly minimum of I_{nt}s fluctuates between Tuesday and Friday, exhibiting discernible trends during the increasing and decreasing phases of the pandemic. These findings underline that the weekly cyclic nature of I_{nt} is a natural phenomenon controlled by socio-economic activities, as evidenced by the effect of national holidays' effects and correlations observed between GDP per capitas and HDI with weekly minimums. Notably, as GDP per capita decreases, the weekly minimum tends to shift towards the beginning, indicating the negative impact of GDP per capita on COVID-19 virus propagation.

The observations above provide crucial insights into the time- and environment-dependent propagation of the COVID-19 virus. The environment can broadly be categorized into two main phases: the workplace and close social circles comprising family and friends (Fig. 4.1). Within this framework, three distinct dynamics emerge in the virus's progression over the course of a week (Fig. 4.1).

Early in the week, the depletion of vulnerable individuals within close social circles causes a decline in I_{nt} towards the midweek (Fig. 4.1.a). Simultaneously, infected individuals from these social circles begin transmitting the virus within workplace settings (Fig. 4.1.a).

Consequently, these newly infected individuals contribute to the spread of the virus within new close social circles of family and friends (Fig. 4.1.b). The interplay between declining and rising trends of I_{nt} in depleted and newly affected social circles, respectively, determines the day of the weekly minimum.

During the midweek, following the weekly minimum, I_{nt} begins to rise due to the efficient virus transmission within the new close social circles initiated by individuals infected at work (Fig. 4.1.b). This phase creates a highly effective transmission loop between workplaces and close social circles, depicted by the rising level of virus propagation in Fig. 4.1.b. This period represents the most efficient viral propagation phase.

As the week draws to a close, viral spread in workplaces diminishes during the weekend, temporarily halting the loop until the following week's minimum. However, virus transmission within close social circles persists until vulnerable individuals within those circles are depleted (Fig. 4.1.c).

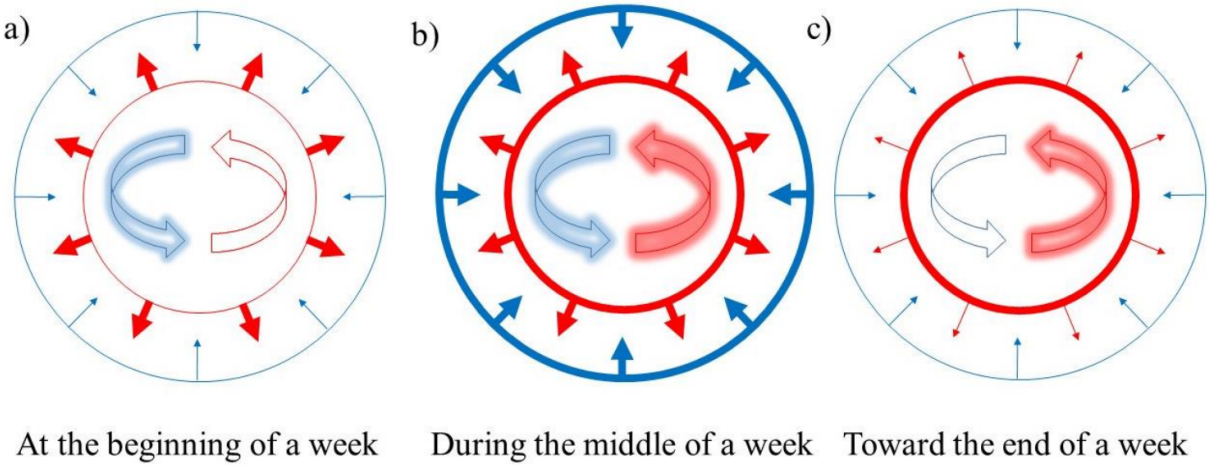

Figure 4.1 Time and environments dependence of SARS-CoV-2 virus transmission model during a week. The daily variation of SARS-CoV-2 virus transmission is represented as circles at the earlier **(a)**, middle **(b)** and later **(c)** days of the week. Blue and red circles represent the transmission in a work and socializing environments, respectively while the thickness of the circles and arrows illustrate the relative transmission rate at different environments, and the origin of the transmitter and the direction of the transmission, respectively. In addition, the intensity of the red and blue glows at the center exhibits the relative intensity of the transmission and the synergistic effect between them.

4.2 Societal Impact and Contribution to Global

It is thought that this master thesis will make a significant contribution to social impact on a global scale. First, better understanding the dynamics of the Covid-19 pandemic by determining the timing of infection provides a solid foundation for healthcare systems around the world. Additionally, the study reveals the relationship between socio-economic factors and virus spread, providing a critical understanding of how epidemics can be managed. In this way, this study will provide a guidance on developing sustainable strategies for similar situations in the future.

Distance measures to be taken in areas where people have intense close contact with each other, such as homes and workplaces, will be the most effective element in global pandemic control. This is of vital importance in terms of protecting social health and welfare, which coincides with the principle of sustainability.

As a result, this thesis provides a new perspective in the fight against possible global health crises that may be encountered in the future, making vital contributions to the management of pandemics and the creation of sustainable health systems. In terms of social impact, it sheds light on the development of data-driven, balanced policies to protect people's health and social lives. This can help be better prepared for similar challenges in the future.

4.3 Future Prospective

The data presented here strongly proves that the transmission of the SARS-CoV-2 virus primarily occurs through close and intimate human interactions which is similar to the observations by the filiation teams. Despite documented instances of viral RNA presence in various room areas and even in air samples within isolated rooms of COVID-19 positive patients, infection mostly results from direct transmission between individuals [63]. This transmission is significantly more efficient at close proximity, especially within the confines of homes and workplaces occurring within a distance of less than one meter [64-66].

Enhanced distancing measures, particularly within close social circles like homes and workplaces, can substantially mitigate the spread of the COVID-19 virus and curb the progression of the pandemic. Simulation models using the $VarR_{0i}$ approach demonstrate that even a modest 11% reduction in virus transmission during specific periods can result in a significant 50% decrease over seven weeks. This underscores the importance of re-evaluating and reinforcing the concept of social distancing among the general population. It's crucial to communicate the unequivocal benefits of appropriate distancing while acknowledging and

minimizing the potential adverse effects of overly stringent social distancing measures on individual psychology. Achieving this balance can effectively limit virus spread while alleviating the burdens of exaggerated social distancing on individuals' mental well-being.

The ability of this newly developed model to calculate daily infections using the Weibull distribution and COVID-19 characteristics sounds like a groundbreaking approach. The identification of a real weekly cycle in daily case numbers and its correlation with socio-economic factors, affecting transmission in working and social environments, is significant. The observation of a variable reproduction number, differing on the pandemic's phases, is also a noteworthy finding.

This pioneering study holds crucial implications, not just for the current COVID-19 pandemic but also for future pandemics. Understanding infection timing and the impact of socio-economic factors on pandemic dynamics is essential for devising effective control strategies, providing invaluable insights for tackling similar outbreaks in the future. In addition, application of this new method is expected to contribute the sustainability of health care systems and labor forces.

BIBLIOGRAPHY

[1] Pal, M., et al., *Severe Acute Respiratory Syndrome Coronavirus-2 (SARS-CoV-2): An Update.* Cureus, 2020. **12**(3).

[2] Ksiazek, T.G., et al., *A novel coronavirus associated with severe acute respiratory syndrome.* N Engl J Med, 2003. **348**(20): p. 1953-66.

[3] Basu-Ray I, A.N., Adeboye A, et al. *Cardiac Manifestations of Coronavirus (COVID-19)*. 2023 Jan 9; Available from: https://www.ncbi.nlm.nih.gov/books/NBK556152/.

[4] Masters, P.S., *The molecular biology of coronaviruses.* Adv Virus Res, 2006. **66**: p. 193-292.

[5] Holmes, K.V., *Coronaviruses (Coronaviridae)*. Encyclopedia of Virology. 1999:291-8. doi: 10.1006/rwvi.1999.0055. Epub 2004 Jun 17.

[6] Almeida, J.D. and D.A. Tyrrell, *The morphology of three previously uncharacterized human respiratory viruses that grow in organ culture.* J Gen Virol, 1967. **1**(2): p. 175-8.

[7] Fehr, A.R. and S. Perlman, *Coronaviruses: an overview of their replication and pathogenesis.* Methods Mol Biol, 2015: p. 2438-7_1.

[8] Gorbalenya, A.E., et al., *Nidovirales: evolving the largest RNA virus genome.* Virus Res, 2006. **117**(1): p. 17-37.

[9] Gorbalenya, A.E., et al., *The species Severe acute respiratory syndrome-related coronavirus: classifying 2019-nCoV and naming it SARS-CoV-2.* Nature Microbiology, 2020. **5**(4): p. 536-544.

[10] Cui, J., F. Li, and Z.L. Shi, *Origin and evolution of pathogenic coronaviruses.* Nat Rev Microbiol, 2019. **17**(3): p. 181-192.

[11] Sahin, A.R., et al., *2019 novel coronavirus (COVID-19) outbreak: a review of the current literature.* EJMO, 2020. **4**(1): p. 1-7.

[12] Hu, B., et al., *Characteristics of SARS-CoV-2 and COVID-19.* Nature Reviews Microbiology, 2021. **19**(3): p. 141-154.

[13] Cherry, J.D. and P. Krogstad, *SARS: The First Pandemic of the 21st Century.* Pediatric Research, 2004. **56**(1): p. 1-5.

[14] Lam, W.K., N.S. Zhong, and W.C. Tan, *Overview on SARS in Asia and the world.* Respirology, 2003. **8**(1): p. 1440-1843.

[15] Memish, Z., et al., *Middle East respiratory syndrome. Lancet Lond Engl 395: 1063–1077*. 2020.

[16] Xu, X.-W., et al., *Clinical findings in a group of patients infected with the 2019 novel coronavirus (SARS-Cov-2) outside of Wuhan, China: retrospective case series.* bmj, 2020. **368**.

[17] Chen, Y., Q. Liu, and D. Guo, *Emerging coronaviruses: Genome structure, replication, and pathogenesis.* J Med Virol, 2020. **92**(4): p. 418-423.

[18] Guarner, J., *Three emerging coronaviruses in two decades: the story of SARS, MERS, and now COVID-19*. 2020, Oxford University Press US. p. 420-421.

[19] Kermack, W.O., A.G. McKendrick, and G.T. Walker, *A contribution to the mathematical theory of epidemics.* Proceedings of the Royal Society of London. Series A, Containing Papers of a Mathematical and Physical Character, 1927. **115**(772): p. 700-721.

[20] Lai, C.-C., et al., *Severe acute respiratory syndrome coronavirus 2 (SARS-CoV-2) and coronavirus disease-2019 (COVID-19): The epidemic and the challenges.* International Journal of Antimicrobial Agents, 2020. **55**(3): p. 105924.

[21] Escandón, K., et al., *COVID-19 false dichotomies and a comprehensive review of the evidence regarding public health, COVID-19 symptomatology, SARS-CoV-2*

transmission, mask wearing, and reinfection. BMC Infect Dis, 2021. **21**(1): p. 021-06357.
[22] Liu, Y., et al., *The impact of non-pharmaceutical interventions on SARS-CoV-2 transmission across 130 countries and territories.* BMC Medicine, 2021. **19**(1): p. 40.
[23] Chiu, N.C., et al., *Impact of Wearing Masks, Hand Hygiene, and Social Distancing on Influenza, Enterovirus, and All-Cause Pneumonia During the Coronavirus Pandemic: Retrospective National Epidemiological Surveillance Study.* J Med Internet Res, 2020. **22**(8): p. 21257.
[24] Pei, S., S. Kandula, and J. Shaman, *Differential effects of intervention timing on COVID-19 spread in the United States.* Sci Adv, 2020. **6**(49).
[25] Khailaie, S., et al., *Development of the reproduction number from coronavirus SARS-CoV-2 case data in Germany and implications for political measures.* BMC Medicine, 2021. **19**(1): p. 32.
[26] Tian, H., et al., *An investigation of transmission control measures during the first 50 days of the COVID-19 epidemic in China.* Science, 2020. **368**(6491): p. 638-642.
[27] Imai, N., et al., *Adoption and impact of non-pharmaceutical interventions for COVID-19.* Wellcome Open Research, 2020. **5**.
[28] Suryawanshi, Y.N. and D.A. Biswas, *Herd Immunity to Fight Against COVID-19: A Narrative Review.* Cureus, 2023. **15**(1).
[29] Barnby, E., M. Reynolds, and J. Gordon, *Reaching Herd Immunity During the SARS-CoV-2 Pandemic: What School Nurses Need to Know.* NASN School Nurse, 2022. **37**(1): p. 13-18.
[30] Hadj Hassine, I., *Covid-19 vaccines and variants of concern: A review.* Rev Med Virol, 2022. **32**(4): p. 9.
[31] Keyel, A.C., et al., *SARS-CoV-2 vaccine breakthrough by Omicron and Delta variants, New York, USA.* Emerging infectious diseases, 2022. **28**(10): p. 1990.
[32] Ka-Wai Hui, E., *Reasons for the increase in emerging and re-emerging viral infectious diseases.* Microbes and Infection, 2006. **8**(3): p. 905-916.
[33] Tregoning, J.S., et al., *Progress of the COVID-19 vaccine effort: viruses, vaccines and variants versus efficacy, effectiveness and escape.* Nature reviews immunology, 2021. **21**(10): p. 626-636.
[34] Pollard, A.J. and E.M. Bijker, *A guide to vaccinology: from basic principles to new developments.* Nature reviews immunology, 2021. **21**(2): p. 83-100.
[35] Subbarao, K., *The success of SARS-CoV-2 vaccines and challenges ahead.* Cell Host Microbe, 2021. **29**(7): p. 1111-1123.
[36] Falahi, S. and A. Kenarkoohi, *Host factors and vaccine efficacy: Implications for COVID-19 vaccines.* J Med Virol, 2022. **94**(4): p. 1330-1335.
[37] Amicone, M., et al., *Mutation rate of SARS-CoV-2 and emergence of mutators during experimental evolution.* Evol Med Public Health, 2022. **10**(1): p. 142-155.
[38] Zhou, B., et al., *SARS-CoV-2 spike D614G change enhances replication and transmission.* Nature, 2021. **592**(7852): p. 122-127.
[39] Ahmad, A., M.A.M. Fawaz, and A. Aisha, *A comparative overview of SARS-CoV-2 and its variants of concern.* Infez Med, 2022. **30**(3): p. 328-343.
[40] Ren, X., et al., *Reinfection in patients with COVID-19: a systematic review.* Global Health Research and Policy, 2022. **7**(1): p. 12.
[41] Wang, Q., et al., *Alarming antibody evasion properties of rising SARS-CoV-2 BQ and XBB subvariants.* Cell, 2023. **186**(2): p. 279-286.
[42] Tartof, S.Y., et al., *Effectiveness of mRNA BNT162b2 COVID-19 vaccine up to 6 months in a large integrated health system in the USA: a retrospective cohort study.* Lancet, 2021. **398**(10309): p. 1407-1416.

[43] Nuwarda, R.F., et al., *Vaccine Hesitancy: Contemporary Issues and Historical Background.* Vaccines, 2022. **10**(10).
[49] Dasic, B., et al., *Human development index in a context of human development: Review on the western Balkans countries.* Brain Behav, 2020. **10**(9): p. 9.
[45] Sitthiyot, T. and K. Holasut, *A simple method for measuring inequality.* Palgrave Communications, 2020. **6**(1): p. 112.
[46] Metcalf, C.J.E., B.T. Grenfell, and A.L. Graham, *Disentangling the dynamical underpinnings of differences in SARS-CoV-2 pathology using within-host ecological models.* PLoS Pathog, 2020. **16**(12).
[47] Cecil, W.T., *COVID-19: daily fluctuations, a weekly cycle, and a negative trend.* Am J Manag Care, 2020. **26**(7): p. 284-285.
[48] Furuse, Y., et al., *Relationship of Test Positivity Rates with COVID-19 Epidemic Dynamics.* Int J Environ Res Public Health, 2021. **18**(9).
[49] Bergman, A., et al., *Oscillations in U.S. COVID-19 Incidence and Mortality Data Reflect Diagnostic and Reporting Factors.* mSystems, 2020. **5**(4): p. 00544-20.
[50] Linton, N.M., et al., *Incubation period and other epidemiological characteristics of 2019 novel coronavirus infections with right truncation: a statistical analysis of publicly available case data.* Journal of clinical medicine, 2020. **9**(2): p. 538.
[51] Li, Y., et al., *The temporal association of introducing and lifting non-pharmaceutical interventions with the time-varying reproduction number (R) of SARS-CoV-2: a modelling study across 131 countries.* Lancet Infect Dis, 2021. **21**(2): p. 193-202.
[52] Lauer, S.A., et al., *The Incubation Period of Coronavirus Disease 2019 (COVID-19) From Publicly Reported Confirmed Cases: Estimation and Application.* Ann Intern Med, 2020. **172**(9): p. 577-582.
[53] Ricon-Becker, I., et al., *A seven-day cycle in COVID-19 infection and mortality rates: Are inter-generational social interactions on the weekends killing susceptible people.* medRxiv, 2020.
[54] Nason, G.P., *COVID-19 cycles and rapidly evaluating lockdown strategies using spectral analysis.* Sci Rep, 2020. **10**(1): p. 020-79092.
[55] Meidan, D., et al., *Alternating quarantine for sustainable epidemic mitigation.* Nat Commun, 2021. **12**(1): p. 020-20324.
[56] Derakhshan, M., H.R. Ansarian, and M. Ghomshei, *Temporal variations in COVID-19: an epidemiological discussion with a practical application.* Journal of International Medical Research, 2021. **49**(8): p. 03000605211033208.
[57] Mitchell, R.N. and J. Zhang, *Four-month intrinsic viral cycle in COVID-19*. Innovation (Camb). 2022 Jan 25;3(1):100196. doi: 10.1016/j.xinn.2021.100196. Epub 2021 Dec 14.
[58] Lawless, J.F., *Basic concepts and models 1.1.* statistical models and methods for lifetime data, 2003: p. 1-47.
[59] Khan, S.A., *Exponentiated Weibull regression for time-to-event data.* Lifetime data analysis, 2018. **24**(2): p. 328-354.
[60] Hu, M., et al., *Risk of Coronavirus Disease 2019 Transmission in Train Passengers: an Epidemiological and Modeling Study.* Clin Infect Dis, 2021. **72**(4): p. 604-610.
[61] Meyerowitz, E.A., et al., *Transmission of SARS-CoV-2: A Review of Viral, Host, and Environmental Factors.* Ann Intern Med, 2021. **174**(1): p. 69-79.
[62] Koelle, K., et al., *The changing epidemiology of SARS-CoV-2.* Science, 2022. **375**(6585): p. 1116-1121.
[63] Santarpia, J.L., et al., *Aerosol and surface contamination of SARS-CoV-2 observed in quarantine and isolation care.* Scientific Reports, 2020. **10**(1): p. 12732.

[64] Ong, S.W.X., et al., *Air, Surface Environmental, and Personal Protective Equipment Contamination by Severe Acute Respiratory Syndrome Coronavirus 2 (SARS-CoV-2) From a Symptomatic Patient.* Jama, 2020. **323**(16): p. 1610-1612.
[65] Bar-On, Y.M., et al., *SARS-CoV-2 (COVID-19) by the numbers.* Elife, 2020. **2**(9): p. 57309.
[66] Dupraz, J., et al., *Prevalence of SARS-CoV-2 in Household Members and Other Close Contacts of COVID-19 Cases: A Serologic Study in Canton of Vaud, Switzerland.* Open Forum Infect Dis, 2021. **8**(7).

CURRICULUM VITAE

2017 – 2022	B.Sc., Molecular Biology and Genetics, Abdullah Gul University, Kayseri, TURKEY
2022 – Present	M.Sc.,Bioengineering, Abdullah Gül University, Kayseri, TURKEY